AD NUMBER

AD862121

NEW LIMITATION CHANGE

TO

Approved for public release, distribution unlimited

FROM

Distribution authorized to U.S. Gov't. agencies and their contractors; Administrative/Operational Use; APR 1968. Other requests shall be referred to Naval Electronics Laboratory Center, San Diego, CA 92152.

AUTHORITY

USNELC ltr, 22 Aug 1974

NELC TECHNICAL DOCUMENT 20
TD 20 (Rev.)

A GUIDE TO DIGITAL COMPUTATATION AND USE OF POWER SPECTRA AND CROSS-POWER SPECTRA

E. E. Gossard and V. R. Noonkester
Radio Physics Division

3 November 1967
(Revised April 1968)

NAVAL ELECTRONICS LABORATORY CENTER
For Command Control and Communications
San Diego, California 92152

FOREWORD

This document replaces NEL Technical Memorandum 600, *A Review of Power Spectrum and Cross Analysis by Digital Methods*, 15 April 1963, which was a compilation of lecture notes on power-spectrum analysis by Dr. E. E. Gossard. The information has been reorganized and expanded. Illustrations and pertinent literature references have been added.

REVERSE SIDE BLANK

CONTENTS

ILLUSTRATIONS

Illustrations (Continued)

REVERSE SIDE BLANK

INTRODUCTION

Complicated interactions of physical processes often occur in nature and their recorded measurements appear random or pseudorandom in character. Such records occur especially often in dealing with atmospheric turbulence or broadband wave phenomena. The medium is usually far too complicated to be predicted or even described in detail.

The autocorrelation function was first used as an independent variable in geophysical problems by G. I. Taylor[1] in his studies of turbulence. It represented an important advance in studying complicated physical processes and forms the basis of modern turbulence theory. The notions of Taylor were extended and explored by Von Karmen and others. The mathematical theory relating correlation functions and spectra has been examined in detail by Wiener.[2]

The usefulness of the cross or autocorrelation function is based on the fact that the statistical character of an extremely complicated record may often be described by a rather simple correlation function (Gaussian, Markov, etc.). While details of the notion are not considered, much more information is available than if only such parameters as the mean or the variance were considered.

Blackman and Tukey[3] have formulated the general problem of spectrum analysis of digital samples and provided quantitative guidance in estimating confidence levels of the analyses.

In recent years, cross-spectrum analysis has been applied extensively in several branches of geophysics and has proved to be a powerful tool for studying certain types of problems. This technique has been effective in the study of atmospheric turbulence[4] and the refractive-index structure of the atmosphere.[5] Munk, Snodgrass, and Tucker[6] have applied cross-spectrum techniques extensively in angle-of-arrival and coherence studies of ocean waves.

Description of the methodology of spectrum and cross-spectrum analysis and its application is widely scattered through the literature of several disciplines. It is our purpose to bring together in one document

---

[1] Superscript numbers identify references listed at end of report.

all of the digital formulation required by most engineers and applied physicists. Elementary derivations of the basic formulae are given. The various errors that may contaminate the analysis are discussed together with the confidence limits applicable to samples of finite length. Examples are given illustrating the application and the step-by-step procedure for obtaining spectra and cross spectra. Two very different applications of cross-spectrum analysis are described, and the significance of cross-power and coherence is discussed.

POWER SPECTRUM ANALYSIS - GENERAL

The straightforward way to obtain the power for a continuous (noise) process, $x(t)$, would be to simply Fourier-analyze the data sample. Thus

$$E(\omega) \overset{T^* \to \infty}{=} \frac{1}{2T^*}\left\{\left[\int_{-T^*}^{T^*} x(t)\cos\omega t\,dt\right]^2 + \left[\int_{-T^*}^{T^*} x(t)\sin\omega t\,dt\right]^2\right\} \quad (1)$$

where the total sample length is $2T^*$.

If we digitize $x(t)$ with the reading interval Δt, we can in principle compute $T^*/\Delta t$ harmonics from the sample and the bandwidth is therefore $(2T^*)^{-1}$. As T^* is increased, the bandwidth correspondingly decreases and although the total amount of data is increased, the information content in the bandwidth remains the same. Therefore the scatter of spectral ordinates is not reduced and we find the surprising result that increasing the sample length does not improve the reliability of our spectral estimate. The problem, then, is to find a way of getting a smooth, reliable estimate of the spectrum of the population and to be able to state confidence limits for the estimates. There are two ways of doing this. We might carry out the harmonic analysis, computing the amplitude of the individual harmonics as just described, and then smooth the spectrum by some algebraic smoothing process. This would be the equivalent of drawing a smooth curve through the points. Alternatively we might carry out the harmonic analysis

of the autocorrelogram. The first method is time-consuming and laborious, and in practice the best method is usually to carry out a harmonic analysis of the autocorrelogram. The spectral bandwidth in the analysis is then $(2\tau_m)^{-1}$ where τ_m is the maximum time lag in the correlation analysis. The bandwidth therefore remains constant (for a given total lag) and, as the sample is increased, more and more statistical information is included in each frequency band leading to a corresponding improvement in the spectral estimates.

THE COVARIANCE FUNCTION

The power spectrum is obtained from the auto-covariance function, and the cross-power spectrum from the cross-covariance function. For two continuous functions $x(t)$ and $y(t)$ whose average is zero the covariance function is defined to be

$$R_{xy}(\tau) = \overline{x(t)\ y(t+\tau)} \overset{T^* \to \infty}{=} \frac{1}{2T^*} \int_{-T^*}^{T^*} x(t)\ y(t+\tau)\ dt \qquad (2)$$

where $2T^*$ is the record length, the bar represents the mean, and τ is the time lag of x relative to y. The function $R(\tau)$ is obtained by letting τ vary from 0 to some maximum value τ_m . If the records are obtained by sampling at an interval Δt, equation 2 is approximated by

$$R(p) = \frac{1}{N-p} \sum_{i=1}^{i=N-p} x_i y_{i+p} \qquad (3)$$

where p is now an integral number of Δt steps and i is the sequential number in the sample ranging from 1 to N.

If the auto-covariance is computed, $x(t)$ and $y(t)$ are identical and

$$R(p) = \frac{1}{N-p} \sum_{i=1}^{i=N-p} x_i x_{i+p} \qquad (4)$$

In this case $R(p)$ is symmetrical around $p = 0$ and only one side of the correlation function need be calculated. When two records are involved both positive and negative values of p are required, and p must take all integral values $0, \pm 1, \pm 2, \ldots \pm m$. The delay time τ is given by $p\Delta t$ and the maximum delay time τ_m is $m\Delta t$. For a fixed m, τ_m decreases as Δt decreases.

POWER-SPECTRUM COMPUTATION

For a continuous covariance function $R(\tau)$ the power spectrum $E(\omega)$ is given by the relation

$$E(\omega) = \frac{2}{\pi} \int_0^\infty R(\tau) \cos \omega\tau \, d\tau \tag{5}$$

where ω is $2\pi f$ and f is cycles per unit time.

When $R(\tau)$ is obtained by sampling a record at intervals Δt, the power spectral estimate $E(h)$ is

$$E(h) = \frac{2\delta}{m} \sum_{p=0}^{p=m} R(p) \cos \frac{\pi p h}{m} \tag{6}$$

where

$$\delta = \begin{cases} \frac{1}{2} \text{ when } p = 0, m \\ 1 \text{ when } 0 < p < m \end{cases}$$

and $h = 0, 1, 2, \ldots m$. The frequency in cycles per unit time associated with the spectral estimate at h is given by

$$f \quad \frac{h}{2m\Delta t} \tag{7}$$

The frequency bandwidth Δf in cycles for each h is f/h or

$$\Delta f = \frac{1}{2m\Delta t} \tag{8}$$

Thus, $E(f)$, the energy in a bandwidth of one cycle, is related to $E(h)$ as

$$E(f) = 2m\Delta t\, E(h) \tag{9}$$

Systematic Errors

Two systematic errors in $E(h)$ arise because of truncation. First, the covariance function is terminated at $p = m$. Secondly, the sample is truncated because it is finite.

The termination of $R(p)$ at $p = m$ creates "corner effects" in equation 5 and produces sidebands in $E(h)$. This is partially avoided by forcing $R(\tau)$ to zero at $p = m$ by multiplication of $R(p)$ in equation 5 by $\left(1 + \cos\frac{\pi p}{m}\right)$.

The other truncation error arises because of the truncation of the sample itself and is a result of the finite sample length. Thus there are artificial abrupt steps in practically every data sample subjected to correlation analysis, and transients are introduced which can contaminate the spectrum. Prefiltering of the records to remove frequencies lower than those being analyzed can reduce this effect but it cannot be entirely eliminated. Furthermore the beginning and end of the sample should be chosen near zero values of the variate to minimize the end effects. However truncation is removed only from the zero order lag and will appear in subsequent lags. In spectrum analysis, truncation error is often the limiting factor and even for large sample sizes it will usually limit the validity of the spectrum to frequencies whose spectral density is within five or six orders of magnitude of the maximum spectral density in the spectrum.

If the spectral density varies rapidly with frequency, the energy contributed to the spectrum by the side-lobes of the spectral window on the low-energy side of the center frequency will be greater relative

to the true spectrum than that contributed by the lobe on the high-energy side. The effect is to shift energy in the true spectrum toward lower-energy regions in the spectrum. It may therefore be advisable to arrange the sample so that the energy is more or less evenly distributed through the spectrum before carrying out the actual analysis. This is sometimes called "prewhitening." One method of prewhitening[6] modifies the data sample x_i in the following way. Let

$$y_i = x_i + b\, x_{i-1} \tag{10}$$

where b lies between +1 and –1. Consider one Fourier component, $x_i = C \cos \frac{2\pi\Delta t}{T} i$. Then

$$x_{i-1} = C \cos \frac{2\pi\Delta t}{T} (i-1) \tag{11}$$

and y_i represents a sum of the form

$$\frac{y_i}{C} = a \cos\left(\frac{2\pi\Delta t}{T} i + \alpha\right) + b \cos\left(\frac{2\pi\Delta t}{T} i - \beta\right) \tag{12}$$

where $a = 1$, $\alpha = 0$, and $\beta = -\frac{2\pi\Delta t}{T}$. The amplitude of y is the resultant of the sum of two vectors of magnitude a, b and phases α, β so

$$\left(\frac{y_i}{C}\right)^2 = a^2 + b^2 + 2ab \cos(\alpha - \beta) \tag{13}$$

Therefore the filter response of this prewhitening scheme is

$$F^2 = 1 + b^2 + 2b \cos \frac{2\pi}{T} \Delta t \tag{14}$$

If $T = \infty$, $F = 1 + b$. If $T = 2\,\Delta t$ (the highest frequency in the analysis), $F = 1 - b$. Therefore, if $b = -0.75$, the energy at high frequencies is increased by a factor of 49/16 and the energy at low frequencies is decreased to 1/16 its actual value.

The effects of averaging within each data point must also be considered. The time series is devoid of the highest frequencies if the observations are from averaged data. In other words, averaging acts like a low-pass filter. The nature of this filter function is well known. If $E(f)$ is the spectrum of some variable x, the spectrum of the mean x averaged over a period t_a is given by

$$E_{\bar{x}}(f) \quad E_x(f) \left(\frac{\sin \pi f t_a}{\pi f t_a}\right)^2 \tag{15}$$

Therefore it is easy to obtain the spectrum of x if the spectrum of $\bar{x}$ is known.

Tukey coined the phrase "aliasing" for the phenomenon that causes energy from one frequency to appear under the "alias" of another frequency. The effect is due to the discrete sampling or digitizing of records for analysis by digital computer. The highest frequency in the analysis has a period twice that of the sampling interval. However, if higher frequencies are present in the record, these higher frequencies may still appear in the analysis but disguised as a lower frequency. Consider the following figure:

Suppose that this sinusoidal record of frequency f is sampled at the points circled. Then the highest frequency in the spectrum analysis, $(2\Delta t)^{-1}$, will be about half the frequency prominent in the record. However, since the sampling interval Δt is a little less than the wavelength in the record, the sampling points fall first on the crests, later in the troughs, then again on the crests producing the dashed curve of frequency $f - (\Delta t)^{-1}$. The original record contained no such frequency. Instead, it was introduced artificially by the large spacing between observations. Frequencies higher than those analyzed appear under the alias of the lower frequency $f - (\Delta t)^{-1}$, and resemble a modulation not unlike a "beating" of the frequencies f and $(\Delta t)^{-1}$. The effect of aliasing is most pronounced at the

high-frequency end of the spectrum. Therefore, one method of minimizing the effects of aliasing is to "over-sample" the record and then ignore the higher spectral ordinates.

Random Errors

Random errors due to finite sampling must also be considered. Different samples from the population would lead to different spectral estimates, each representing a summation over the harmonics in the sample. If samples are drawn at random from a statistically stationary record and if the variate is normally distributed, the spectral estimate for a given frequency will vary about the population spectrum according to the chi-square distribution which is widely tabulated. The value of chi-square for a given significance depends only on the number of degrees of freedom, which is defined as the number of independent normally distributed quantities that are summed -- in our case the number of harmonics in the summation. The effective width of the main lobe of the window of the Tukey filter (Hanning function) is 2. Since this will pass N/m harmonics through each of the two windows, the number of degrees of freedom is approximately $2N/m$. Actually, Tukey suggests that the number of degrees of freedom, ν, is more like $2.5(N/m)-1/2$ but he recommends the use of $2(N/m)-1/2$ because of uncertainties such as the assumption of a normal distribution of the variate, the appropriateness of the chi-square distribution, and the statistical stationarity of the record. The confidence limits for the spectral ordinates are related to the degrees of freedom in figure 1.

It is evident that the confidence limits depend directly on sample size, N, and on the total amount the record is lagged, m. The expression $2(N/m)-1/2$ relating degrees of freedom to sample size and total lag is important, and several things can be immediately pointed out. First of all, when the sample size is large compared to the total lag, ν is nearly proportional to the ratio of sample size, N, to maximum lag length, m. Therefore this ratio is the important factor in determining the confidence limits of the spectrum analysis. Furthermore, the maximum lag, τ_m, determines the lowest frequency (longest period) that can be analyzed in the data

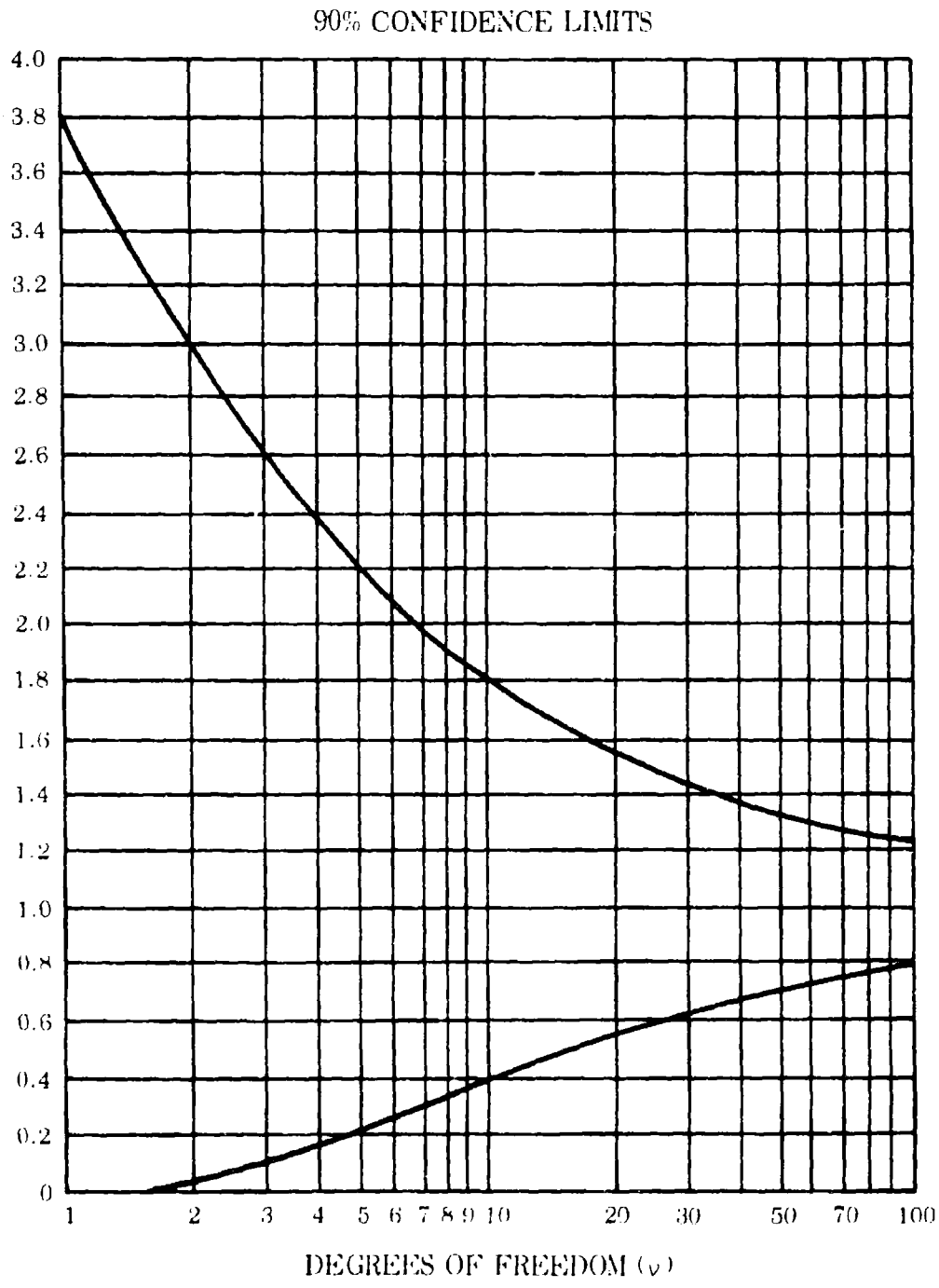

Figure 1. Ninety percent confidence limits relating degrees of freedom to the ratio of computed energy to true energy density. Nine times out of ten the computed spectral density will lie between the curves when expressed as a ratio to the correct population density. (After Blackman and Tukey; see ref. 3.)

sample since $f_{min} = (2\tau_m)^{-1}$, while the digitizing interval, Δt, determines the highest frequency since $f_{max} = (2\Delta t)^{-1}$. This means that the lowest frequency of interest in the analysis determines the sample length, $2T^*$, required in order to obtain a satisfactory confidence level in the spectrum analysis. This is a point to be emphasized because sometimes attempts are made to get increased reliability by just sampling the record more often to get a larger N without increasing T^*. The sampling frequency determines the highest frequency capable of detection in the record just as the maximum lag (time) determines the lowest frequency. Since the highest frequency in the spectrum will be $(2\Delta t)^{-1}$, increasing the sampling rate (that is decreasing the sampling interval Δt) simply extends the analysis to higher frequencies and the confidence limits of the spectrum remain unchanged if T^*/τ_m is unchanged.

Stationarity and Filtering

The foregoing discussion has pointed out the adverse effects produced by frequencies outside the range of those being considered in the spectrum analysis. They lead to errors from aliasing and to erroneous confidence estimates related to nonstationarity.

A sample must be stationary if it is to be considered representative of the population. Stationarity normally means that the lower-order statistics should not vary throughout the record. If the mean and variance of the record are constant everywhere in the record it is generally considered stationary. Consider the record $\overline{fE}$ shown at the top of figure 2. $\overline{fE}$ is an average of fE about local noon and indicates the average ionospheric electron density.* The record gives $\overline{fE}$ for 180 days and contains a gradual decrease in the running average (averaged over five to ten days) which is caused by the annual change in the solar zenith angle. Thus the record of $\overline{fE}$ is not stationary relative to the mean, the first-order statistic.

---

* fE is the critical frequency for radio penetration of the E Region of the ionosphere.

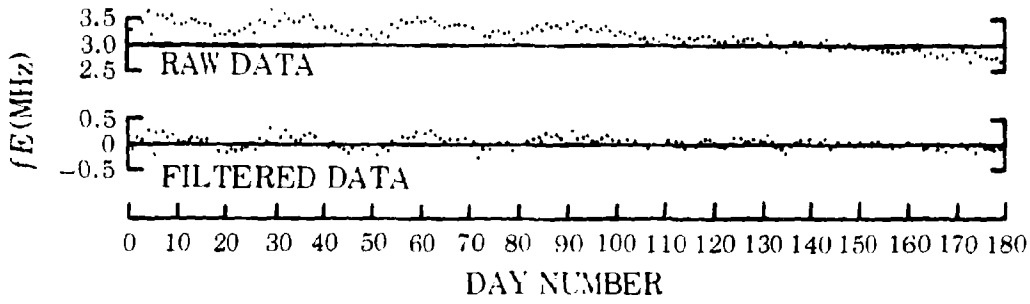

Figure 2. A portion of a record of fE (see text for definition). The upper record is the unfiltered raw data; the lower record is data filtered using equation A-7 with $m = 100$ days.

If the record of $\overline{fE}$ extended over four years, four annual cycles would be present. The record should not be considered stationary because 10 to 20 cycles at the lowest frequency in a record is considered necessary for stationarity.

An eleven-year record of $\overline{fE}$ would show a longer-period variation associated with the 11-to-12-year sunspot cycle, and again the record would be nonstationary. Further extension of the record might reveal longer-period variations which might be associated with climatic changes. Most geophysical data are correspondingly nonstationary and should be converted to a stationary form relative to the mean. Nonstationarity in the mean can be removed by numerically prefiltering the data as shown by the bottom record of figure 2.

Some data show a change of variance throughout the record and the record is considered nonstationary. Nonstationarity in the variance cannot be removed by prefiltering. Unless the variation is judged to be excessive by some method, the nonstationarity of the variance is usually ignored. Nonstationarity in the variance or other higher-order statistic will not be considered here.

Low- or high-frequency components in a record may be removed by mechanical-electrical devices during recording or by mathematical methods after recording. Inductors or capacitors are often used to remove low frequencies and a time constant may be introduced by an RC circuit to remove high frequencies prior to recording a signal. Various mathematical filters are available for operating on recorded data, depending on what frequencies one desires to remove or reduce in amplitude. The important requirement

is that the frequency response of the filter must be known so that the analysis of the spectral information can be objective. Mechanical or electrical filter responses will not be examined. Examples of two convenient numerical filters are given in Appendix A.

The foregoing discussion of the main elements involved in autocorrelation and power-spectrum analysis leads now to consideration of a simple example.

Sample Problem (Power Spectrum)

Consider the record of geomagnetic fluctuations shown in figure 3. The first step in any spectrum analysis is to decide the range of frequencies of interest. In the present record, it is obvious that we have a strong 60-Hz component. We will therefore wish to terminate the spectrum analysis at a frequency much less than 60 Hz -- say 30 Hz. In this data sample, we are looking for earth-cavity resonance effects. Theory offers some guidance and we know that the fundamental frequency should be some few Hz. We might therefore decide to analyze the spectrum down to a frequency of perhaps 0.5 Hz. This frequency determines the value of τ_m to be used in the analysis. τ_m not only determines the longest period ($2\tau_m$) that we can analyze in the record, but it also determines the resolution in the spectrum analysis ($\Delta f = (2\tau_m)^{-1}$). The smaller the maximum lag, m, compared to the number of observations, N, the more smoothing is obtained in the spectrum. Also, it is important to remember that less computer time is required. However, a small value of m limits the resolution

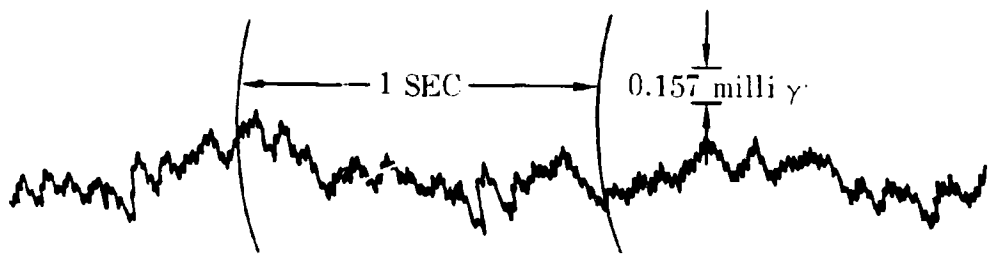

Figure 3. Portion of magnetometer record showing micropulsations of earth's magnetic field. Record is contaminated with 60-cycle "noise".

and may obscure significant characteristics in the spectrum of the population. If we wish to examine frequencies as low as 0.5 Hz, the maximum lag, m, in the correlation analysis must extend over at least a 1-second time interval. At the other end of the spectrum, if we wish to examine frequencies as high as 30 Hz, we must sample the records at twice that frequency, or 60 samples per second. At a sampling rate of 60 Hz, there are 60 lags in a time interval of 1 second, therefore m 60. We have now selected the range of frequencies of interest and the maximum lag number m in the correlation analysis. It remains to determine how long a data sample will be required to achieve the ordinate confidence we require. Suppose we decide that 100 degrees of freedom is adequate. This means that 90 percent of the time the estimated ordinate value will lie between approximately 0.77 and 1.25 of the true spectral value for the population. For 100 degrees of freedom and a lag of 60, we find that our required sample length is 3000. We are now ready to carry out the spectrum analysis. We will usually wish to express the spectral values as the variance of the data per cycle per unit time. That is, if the record is recorded in seconds we will usually wish to express the energy as variance per cycle per second. This has been done in the sample shown and the resulting units are (milli γ)^2/Hz.

In geophysical problems, it often happens that the spectrum falls off rapidly as we proceed toward higher frequencies, and it may in fact drop several orders of magnitude within the range of frequencies analyzed. It is therefore often convenient to plot log E as function of frequency. Alternatively, it may be convenient to multiply each spectral value by its frequency to obtain a spectral function with dimensions of variance and a reduced range of variation. The spectrum can usually then be conveniently plotted on linear paper without the undue suppression of spectral lines that may occur at the higher frequencies. This is the method chosen for presentation in figure 4.

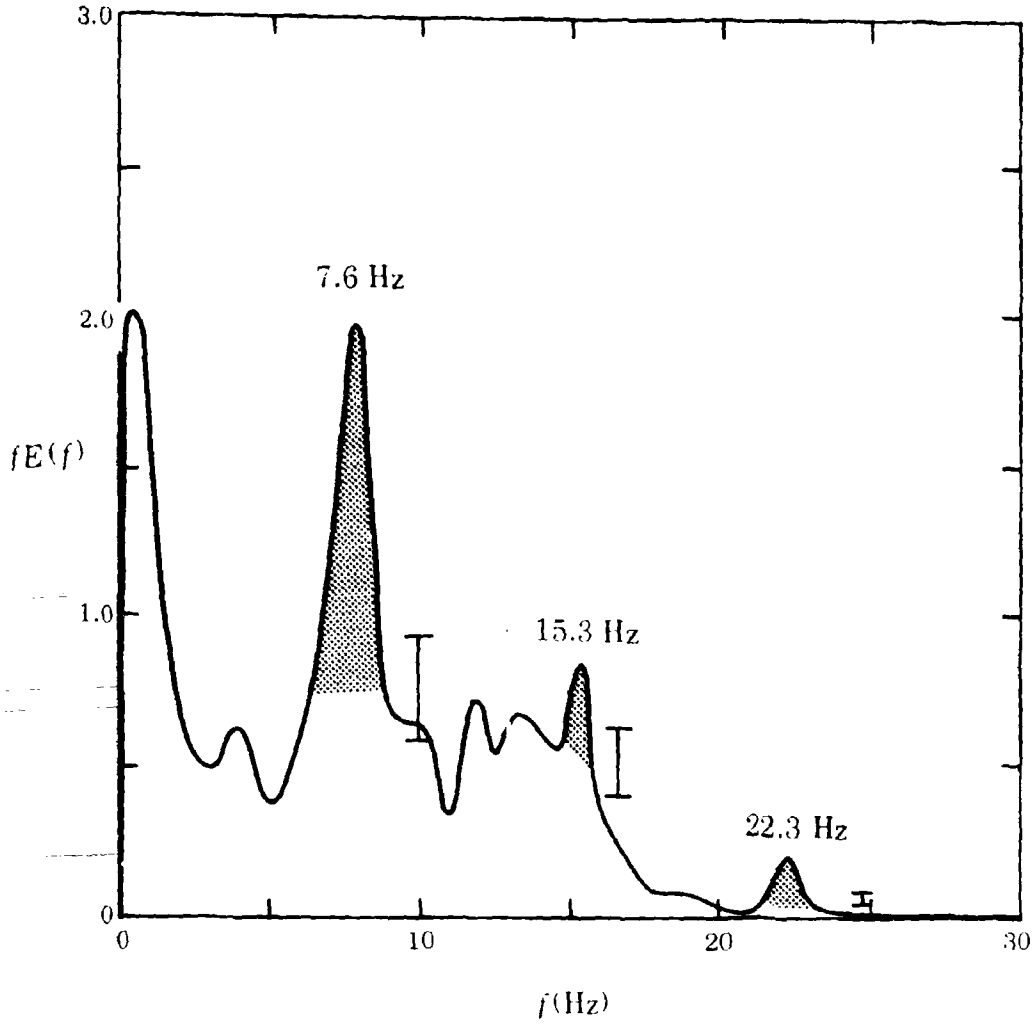

Figure 4. The product of power spectral density and frequency for the magnetometer record shown in figure 3. The brackets indicate confidence limits for 100 degrees of freedom in the analysis. Units of $fE(f)$ are $\text{Hz} \times \frac{(\text{milli}\,\gamma)^2}{\text{Hz}}$

CROSS-SPECTRUM COMPUTATION

The power spectrum provides information about the frequency content of a time series. Cross-spectrum analysis provides information about the relationship between two or more time series in the frequency domain, i.e., the coherence and phase lag. Goodman[7,8] discusses the theory and principles of cross-spectrum analysis. The multiple coherence is analogous to the multiple-correlation coefficient. In a two-parameter analysis the phase lag is analogous to the intercepts of the regression line of best fit in the correlation analysis. Just as significance levels are required in a correlation analysis, confidence levels are also required in cross-spectrum analysis. This section will present some elementary concepts of coherence and phase lag and present some examples in which confidence levels are used.

Just as the power spectrum can be obtained by Fourier-transforming the auto-covariance function, the cross spectrum is obtained by transforming the cross-covariance function. If the cross-covariance function is asymmetrical, both even and odd terms are required to represent it and the cross spectrum will therefore be complex. Therefore

$$E_{12}(\omega) = C - iQ = \frac{1}{\pi}\int_{-\infty}^{\infty} R_{12}(\tau)\exp(i\omega\tau)\,d\tau \tag{16}$$

$$= \frac{2}{\pi}\int_{0}^{\infty} R_{12}(\tau)\cos\omega\tau\,d\tau + i\frac{1}{\pi}\int_{-\infty}^{\infty} R_{12}(\tau)\sin\omega\tau\,d\tau$$

Now $R_{12}(\tau)$ can be decomposed into a symmetric term and an antisymmetric term as

$$R_{12}(\tau) = \frac{R_{12}(\tau) + R_{12}(-\tau)}{2} + \frac{R_{12}(\tau) - R_{12}(-\tau)}{2} \tag{17}$$

where the symmetric and antisymmetric terms are as shown schematically:

Therefore

$$C(\omega) = \frac{2}{\pi}\int_0^{\tau_m} \frac{R_{12}(\tau) + R_{12}(-\tau)}{2} \cos \omega\tau \, d\tau \tag{18}$$

$$Q(\omega) = \frac{1}{\pi}\int_{-\tau_m}^{\tau_m} \frac{R_{12}(\tau) - R_{12}(-\tau)}{2} \sin \omega\tau \, d\tau \tag{19}$$

The smoothed spectral estimates of $C(f)$ and $Q(f)$ at h (corresponding to frequency $f = h/(2m\Delta t)$) can be numerically calculated from

$$C(f) = 2\Delta t \left[R_{12}(0) + \sum_{p=1}^{p=m-1} \frac{R_{12}(p) + R_{12}(-p)}{2}\left(1 + \cos\frac{\pi p}{m}\right)\cos\frac{\pi p h}{m}\right] \tag{20}$$

$$Q(f) = 2\Delta t \left[\sum_{p=1}^{p=m-1} \frac{R_{12}(p) - R_{12}(-p)}{2}\left(1 + \cos\frac{\pi p}{m}\right)\sin\frac{\pi p h}{m}\right] \tag{21}$$

When records 1 and 2 are identical $R_{12} = R_{11} = R_{22}$ is symmetrical about $\tau = 0$, and $C(f)$ becomes the power-spectral estimate while $Q(f)$ vanishes.

The phase relationship between frequencies in records being cross-spectrum analyzed is given by

$$\tan \omega\tau = \frac{Q(\omega)}{C(\omega)} \tag{22}$$

while the cross-power is

$$|E_{12}| \quad \sqrt{C^2 + Q^2} \tag{23}$$

The coherence is defined as the square of the cross-power divided by the product of the powers in the two records being analyzed, or

$$\text{coh}\,(\omega) = \frac{C^2 + Q^2}{E_1 E_2} \tag{24}$$

Coherence measures the fraction of the variance of one variable (record 1) that can be specified by another variable (record 2) because of phase coherence due to some direct or indirect association between the records at frequency ω. The coherence should vary only from 0 to 1, but coherence quickly becomes unreliable if the degrees of freedom in the analysis are insufficient and may even exceed unity if the confidence in the numerical analysis is low.

When more than two records are involved, multiple coherence can be calculated with interpretations similar to multiple-correlation coefficients. Multiple coherence will not be considered here.

There is a subtle difficulty that appears when we work with data of finite length. The problem is very well stated by Madden,[9] as follows:

> *"The cross-correlation of two transients does not lose any of the power of the transients, and this would appear to guarantee a coherency of 1. This difficulty is overcome by making the spectral window average together the cross-power of a group of neighboring frequencies. When the two noise signals are random to each other, the phases of each frequency component are random, and a vector addition of the cross-powers of a group of neighboring frequencies tends to cancel. When the two noise signals are coherent, the phases of each frequency in the cross-power are those of the phase spectrum of the linear operator which generates one signal from the other. If this spectrum is slowly varying as a function of frequency, the addition of neighboring cross-powers does not cancel out. This necessitates some care in evaluating coherency estimates if time delays are involved, or if very sharp frequency structure exists in the relationship between the data."*

The probability of obtaining a particular coherence by chance (the level of confidence) must be specified if the statistical analysis is

to be considered complete. The confidence level implies a reliability level for coherence. The probability density P of coherence has been considered by Goodman[7] and is approximately given by:

$$P(\text{coh}) \quad \frac{2(1-\text{coh}^*)^{\nu/2}}{\Gamma\left(\frac{\nu}{2}\right)\Gamma\left(\frac{\nu}{2}-1\right)}(\text{coh})(1-\text{coh}^2)^{(\nu/2)-2} \times \sum_{h=0}^{\infty} \frac{\text{coh}^{2h}\Gamma^2\left(\frac{\nu}{2}+h\right)(\text{coh}^*)^h}{\Gamma^2(h+1)} \tag{25}$$

where coh* is the population coherence. Alexander and Vok[10] have tabulated the cumulative distribution of sample coherence as a function of the degrees of freedom [$\nu = (2Nm) - 0.5$] and the true or population coherence. Unfortunately, ν ranges from 2 to only 21 in the tables. Population coherence ranges from 0 to 0.99. The true coherence is the coherence expected from the population having ν degrees of freedom. Figure 5 shows the cumulative distribution function of coherence for 5, 10, 15, and 20 degrees of freedom when the population coherence is zero. Figure 6 shows the cumulative distribution function of coherence for population coherences of 0, 5, 10, 15, 20, 30, and 40 when ν is 10. These data were taken from reference 10.

The probability P that phase will lie within a certain increment $\Delta\theta$ is

$$\sin^2\Delta\theta = \frac{1-\text{coh}^*}{\text{coh}^*}\left[(1-P)^{-2/\nu}-1\right] \tag{26}$$

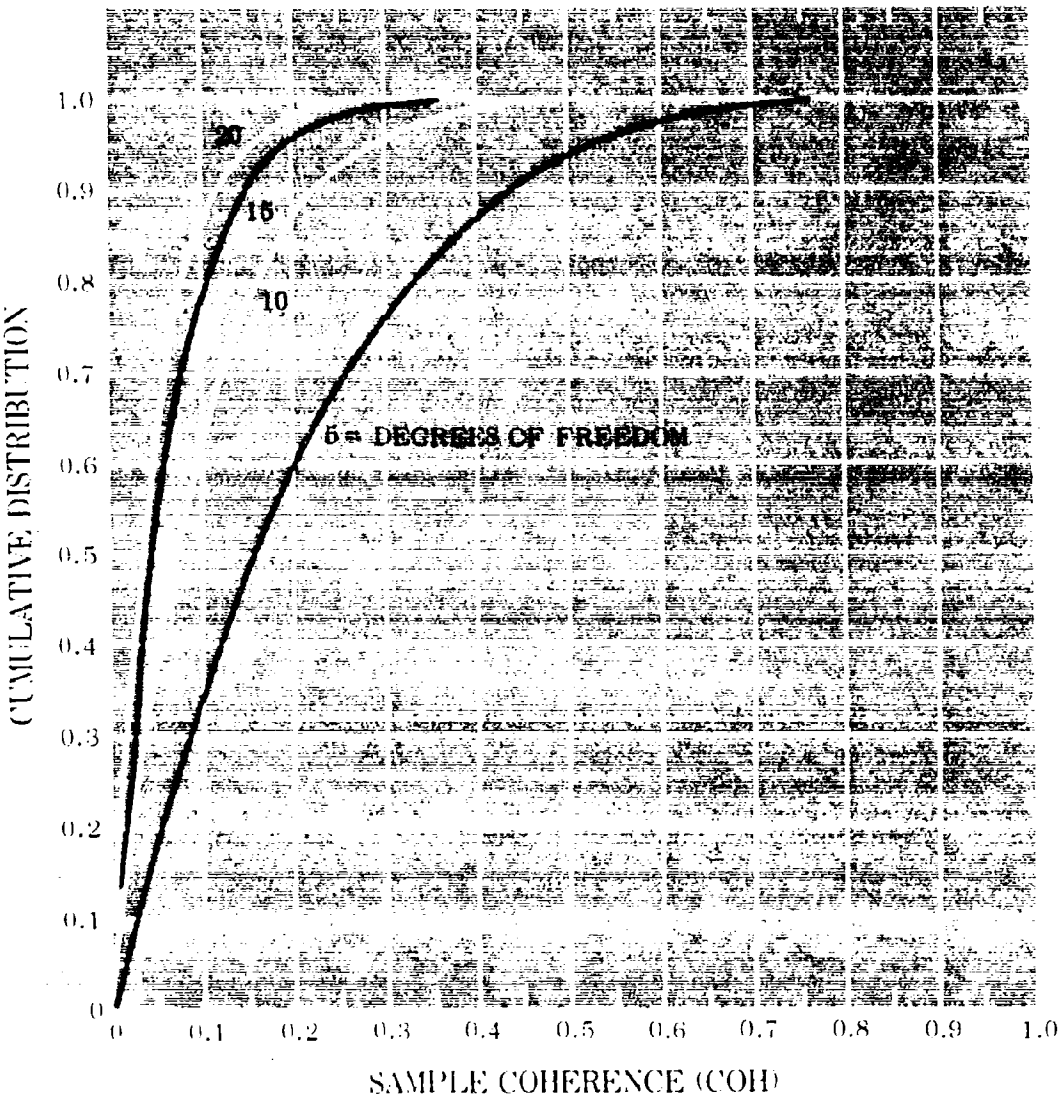

Figure 5. The cumulative distribution of sample coherence as a function of degrees of freedom for a population coherence of zero. (After Alexander and Vok; see ref. 10.)

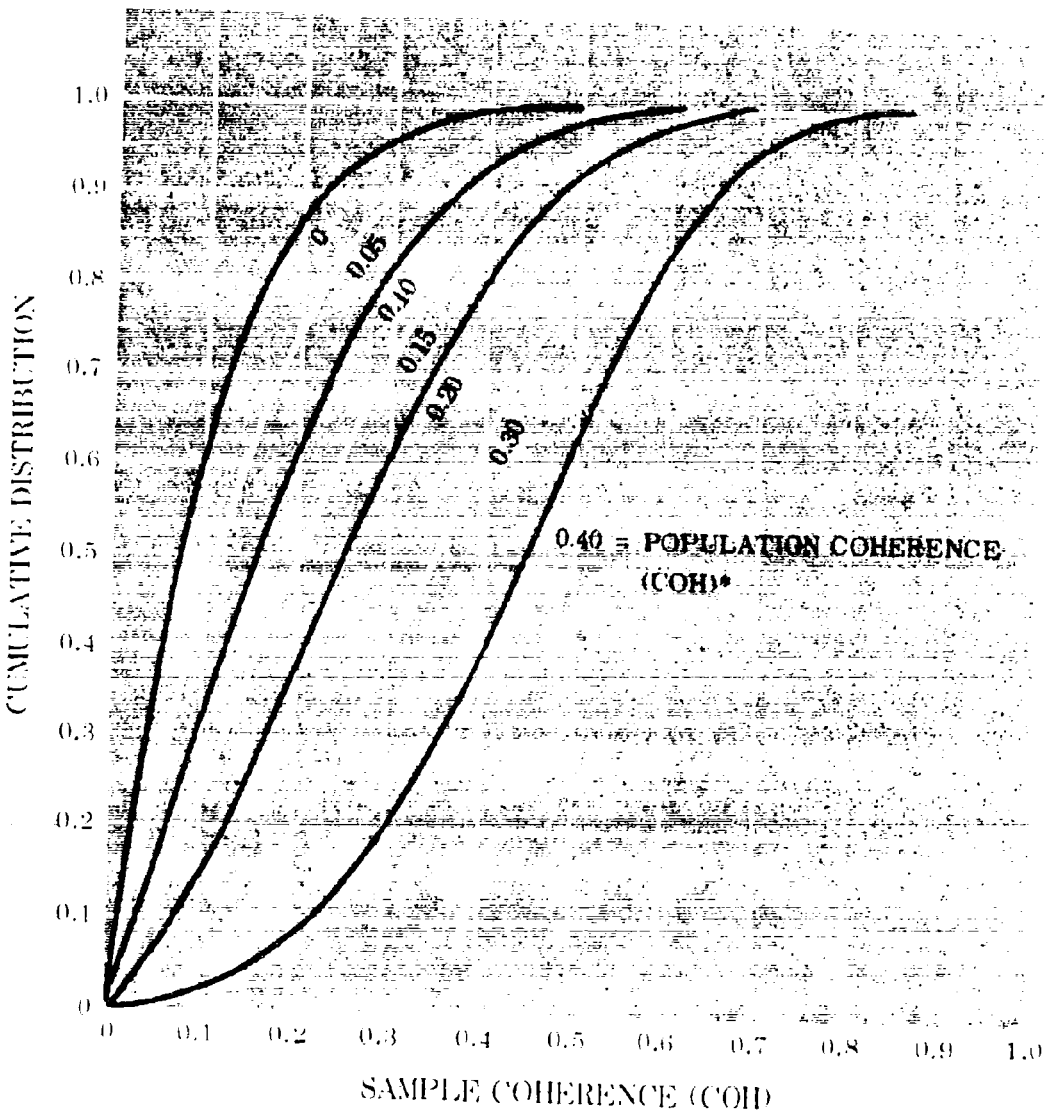

Figure 6. The cumulative distribution of sample coherence as a function of population coherence for 10 degrees of freedom. (After Alexander and Vok, see ref. 10.)

The limits for $P = 0.95$ are shown in figure 7 (taken from ref. 6).

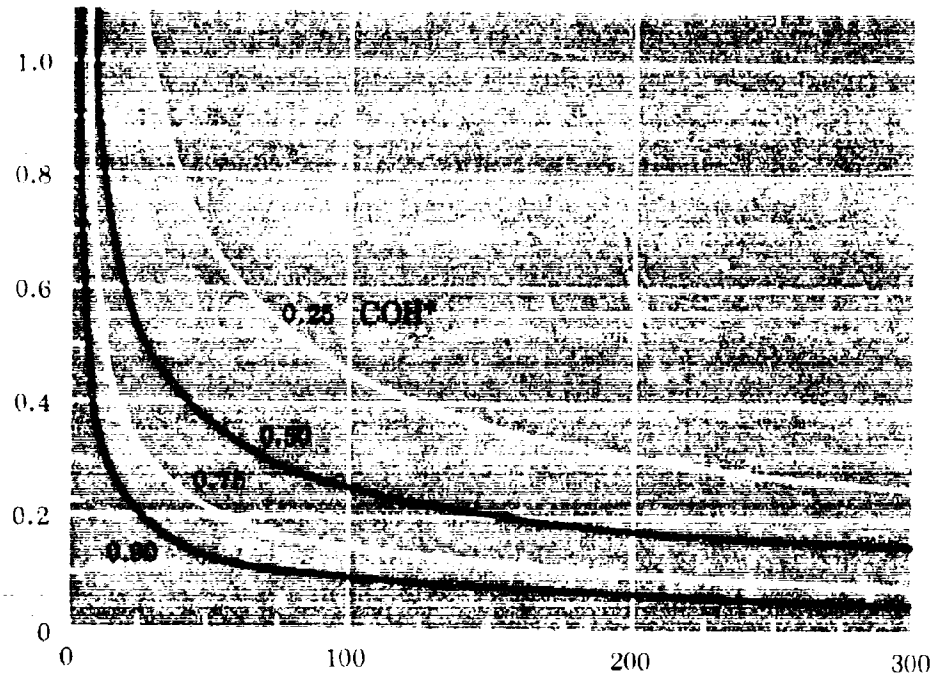

Figure 7. Ninety-five percent confidence limits for phase angles as functions of degrees of freedom, ν. Thus for $\nu = 100$ degrees of freedom there are nineteen chances in twenty if coh* = 0.5 that the true phase is within 0.25 radian of the computed phase. (From Munk *et al.*; see ref. 6.)

Sample Problem Applying Cross-Spectrum Analysis to Time-Related Functions

The electron density in the ionosphere is known to be controlled primarily by the intensity of the solar ionizing energy. Aside from the diurnal and annual variation, the electron density varies with the sunspot number which has a long-term 11-year cycle and a short-term 27-day cycle. A 15-day or semilunar cycle has also been found. A study by Noonkester[11] was made to determine the behavior of two ionospheric layers (E and F) at the 15- and 27-day periods. Daily measures of $\overline{fE}$ and $\overline{fF}$ represent the variation of electron density at the E and F levels. They were obtained for 2722 consecutive days and the annual cycle was removed (see filtered

data in the sample record, fig. 2). The power spectrum and the coherence spectrum were then obtained for $\overline{fE}$ and $\overline{fF}$.

The power spectra of $\overline{fE}$ and $\overline{fF}$ showed a significant maximum near a period of 27 days, but did not show any maximum near the 15-day period. The power spectra of each quarter of the data showed that the 27-day period was dependent on the portion of the records considered.

A coherence spectrum between $\overline{fE}$ and $\overline{fF}$ (fig. 8) showed that they were related near the 27- and 15-day periods. The spectral estimates have 42 degrees of freedom and are separated by 4×10^{-3} cycles/day. The confidence limits cannot be determined from the tables of Alexander and Vok[10] because these tables do not consider ν greater than 21. However, an estimate of the significance level was made at a ν of 21. The population coherence was assumed to be the average of the 125 estimates of coherence in the spectrum. According to the tables, at 21 degrees of freedom a coherence of 0.35 or greater has a probability of less than 0.01 of occurring by chance. Certainly the coherence estimates in figure 8 at the 27- and 15-day periods have a small probability of occurring by chance.

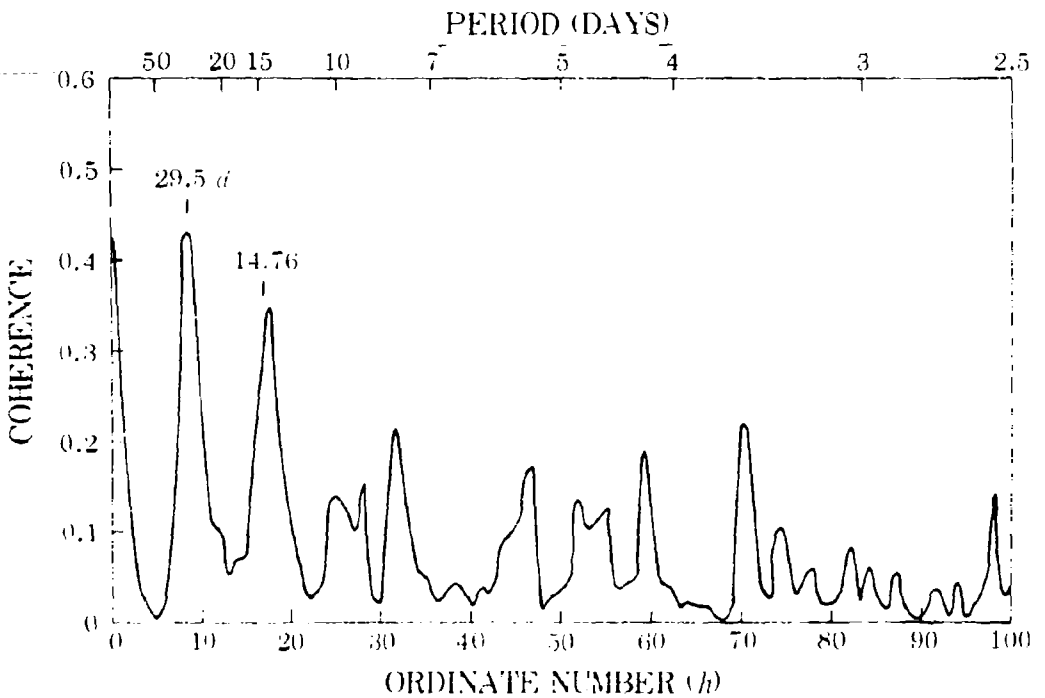

Figure 8. The coherence between fE and fF (see text for definition) as a function of ordinate number or period. The spectral estimates have 42 degrees of freedom and are separated by 4×10^{-3} cycles per day.

The value of the coherence is shown in the above example. The power spectra of $\overline{fE}$ and $\overline{fF}$ indicated that the amplitude of the 15-day period was at the background noise level, but the coherence between these variables indicated that they were related at the 15-day period. Although the amplitude was small at the 15-day period, $\overline{fE}$ and $\overline{fF}$ varied coherently at the 15-day period. This is equivalent to using phase coherence to obtain a signal out of a noisy record.

According to equations 22 and 26, $\overline{fE}$ was found to precede $\overline{fF}$ by 1.2 days near the 27-day period within confidence limits of ± 2.0 days 90 percent of the time. $\overline{fE}$ and $\overline{fF}$ were found to be in phase at the 15-day period and within confidence limits of ± 1.2 days 90 percent of the time.

Application of Cross-Spectrum Analysis to Spatially Separated Recordings

In this application, we consider two separate records of a time-varying function received at two spatially separated stations A_1, A_2 shown schematically in figure 9. The function might be generated by the steady drift across the stations of a spatially varying medium perturbed by turbulent processes; or it might be generated by a wave motion of significant bandwidth propagating through the medium where the different frequency components may propagate in different directions with different velocities. Figure 9A shows the case for a single Fourier component of a wave structure propagating in the x direction. In figure 9A let τ_0 be the time lag between the arrival of the wave crest at A_1 and A_2. From equations 22 and 23

$$C(\omega) = |E_{12}(\omega)| \cos \omega \tau_0 \tag{27}$$

$$Q(\omega) = |E_{12}(\omega)| \sin \omega \tau_0 \tag{28}$$

If $\tau_0 = 0$, $Q(f) = 0$. If τ_0 is not zero, $\tan \omega \tau_0 = Q(\omega)/C(\omega)$ gives the phase lag between the records corresponding to the distance of travel $V \tau_0 \quad L \sin \theta$. Since $\omega \quad (2\pi/\lambda) V \quad kV$, $\tan [(2\pi/\lambda)(L \sin \theta)] \quad Q(f)/C(f)$, so the wavelength, λ, and the average angle-of-arrival, θ (see fig. 9A), can be found as a function of frequency f.

A. GEOMETRY OF WAVE TRAIN OF WAVELENGTH, λ, PASSING RECORDERS LOCATED AT A_1 AND A_2 SEPARATED BY A DISTANCE L. THE LINE JOINING THE STATIONS MAKES THE ANGLE θ WITH THE y AXIS. θ IS THEREFORE THE AVERAGE ANGLE OF PROPAGATION OF THE WAVE TRAIN WITH RESPECT TO THE ORIENTATION OF THE RECORDER PAIRS.

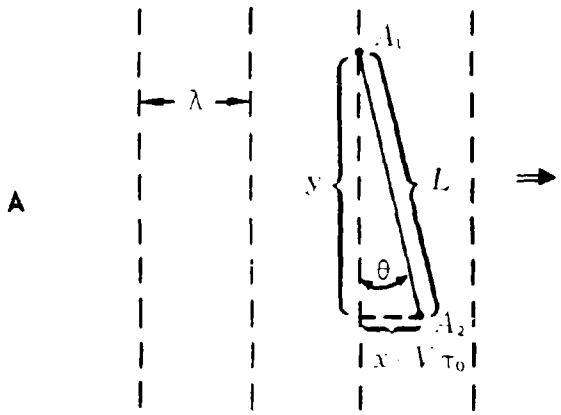

B. GEOMETRY OF TWO INTERFERING WAVE TRAINS WHOSE NORMALS MAKE THE ANGLE φ WITH THE x AXIS. THEY MAKE ANGLES $\theta \pm \varphi$ WITH RESPECT TO THE NORMAL TO THE LINE OF STATION SEPARATION.

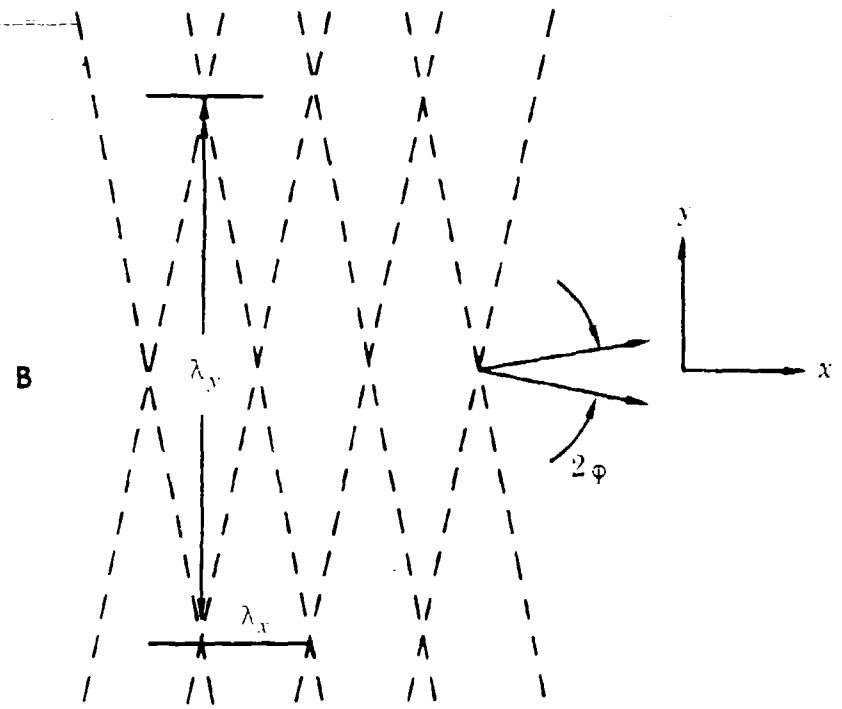

Figure 9. Geometry of wave trains passing spatially separated recording sites.

The co-spectrum $C(f)$ corresponds to the in-phase frequencies of the spectrum, and the quadrature spectrum, $Q(f)$, corresponds to the out-of-phase components. Since the cosine transform (co-spectrum) is an even function, the corresponding correlation function must be symmetric. The correlation function corresponding to the sine transform (quadrature spectrum) is anti-symmetric. Since the autocorrelation function is always symmetric for a stationary time series, the corresponding quadrature spectrum is always zero, and the co-spectrum is identical to the power spectrum. A cross-correlation function is, in general, nonsymmetric about 0, and $Q(f)$ is not zero. The argument $\omega \tau_0$ is then the phase lag between the two records which were cross-correlated and represents the phase cross-spectrum between the records.

The normalized magnitude squared of the cross-spectrum between two records is called the coherence. It is sometimes stated that coherence is like a correlation function representative of a frequency band in the spectrum. This can be a useful concept if used cautiously, but factors that can reduce the coherence between records are now considered.

Suppose we are receiving some signal at two recording sites spatially seperated. Suppose the signal is modulated by temporal changes in the propagation medium and we wish to obtain information about these changes by examining the coherence of the fluctuations in the two records. The coherence will be degraded by:

1. Random or noiselike phenomena such as turbulence in the neighborhood of each recorder.

2. Anything that causes the same frequency to have a variable travel time between the recorders such as a changing direction of propagation during the sampling, or nonlinear processes in wave phenomena.

3. Source or sink located between recorders.

4. The same frequencies coming simultaneously from different directions as would be the case if wavelike phenomena in the medium had a significant "beam width" or a distributed source. Then interference between waves coming from

different directions at the same frequency will "smear" the phase difference between recording stations and reduce the coherence.

The last mechanism is of both theoretical and practical interest and has been used by oceanographers (i.e., Cox; see ref. 12) to study the "beam width" of ocean waves. The problem will now be formulated.

It is clear from the preceding development of the expressions for the cross-spectra that the $\sqrt{\text{coherence}}$ is just the normalized modulus of the complex cross-spectrum and the phase angle, $\omega \tau_0$, is its argument.

Suppose now that waves of the same frequency arrive at the recorders from different directions, $\theta + \varphi$, where θ is the average direction (see fig. 9B). Let the co- and quadrature spectra represent the average of spectral components over all directions of arrival. Then $\omega \tau_0 = kL \sin(\theta + \varphi) = kL(\sin\theta \cos\varphi + \cos\theta \sin\varphi)$. Let x and y be the components of L in, and normal to, the average direction of propagation, respectively. Then from equations 27 and 28 we have

$$C(\omega) = \frac{1}{2\Delta\varphi}\int_{-\Delta\varphi}^{\Delta\varphi} E_{12}(\omega,\varphi)\cos(kx\cos\varphi + ky\sin\varphi)\,d\varphi \qquad (29)$$

$$Q(\omega) = \frac{1}{2\Delta\varphi}\int_{-\Delta\varphi}^{\Delta\varphi} E_{12}(\omega,\varphi)\sin(kx\cos\varphi + ky\sin\varphi)\,d\varphi \qquad (30)$$

Now if we consider the coherence to be degraded only by the interference of waves of the same frequency coming from different directions with differing $\omega \tau_0$, equations 27 and 28 show that $|E_{12}|^2 = E_1 E_2$. Furthermore, if the wave structure is spatially homogeneous, $E_1(\omega, \varphi) = E_2(\omega, \varphi) = E(\omega, \varphi)$. If $E(\omega, \varphi)$ is assumed to be uniform for $-\Delta\varphi < \varphi < +\Delta\varphi$ and zero elsewhere it can be removed from the integral so that equations 29 and 30 give:

$$\frac{(C + iQ)(\omega, \Delta\varphi)}{E(\omega)} = \frac{1}{2\Delta\varphi}\int_{-\Delta\varphi}^{\Delta\varphi} \exp[-ik(x\cos\varphi + y\sin\varphi)]\,d\varphi \qquad (31)$$

Thus coherence, equation 21, which is just the square of the cross-power normalized to the auto powers, can be used as a measure of the "beam width" of wave components.

An alternative concept of the dependence of the cross-power on wave pattern is to define a "radiation pattern" $F(\varphi)$ of the recorder array. Stated formally

$$F(\varphi)\int E(\omega,\varphi)\,d\varphi=\int E(\omega,\varphi)\exp\left[-ik(x\cos\varphi+y\sin\varphi)\right]d\varphi \tag{32}$$

so that

$$F(\varphi)=\frac{\int E(\omega,\varphi)\exp\left[-ik(x\cos\varphi+y\sin\varphi)\right]d\varphi}{\int E(\omega,\varphi)\,d\varphi} \tag{33}$$

where $E(\omega,\varphi)$ is the directional spectrum of the radiation.

If, as before, $E(\omega)$ is constant for $-\Delta\varphi<\varphi<\Delta\varphi$ and zero elsewhere, $E(\omega)$ can be removed from the integral and the limits will be $-\Delta\varphi$ and $\Delta\varphi$ so that

$$F(\Delta\varphi)=\frac{1}{2\Delta\varphi}\int_{-\Delta\varphi}^{\Delta\varphi}\exp\left[-ik(x\cos\varphi+y\sin\varphi)\right]d\varphi \tag{34}$$

and we thus identify $|F(\Delta\varphi)|$ with $\sqrt{\text{coherence}}$ by equation 31. Equation 34 can be written

$$F(\Delta\varphi)=\frac{1}{2\Delta\varphi}\int_{-\Delta\varphi}^{\Delta\varphi}\left[\cos(ky\sin\varphi)-i\sin(ky\sin\varphi)\right]\exp(-ikx\cos\varphi)\,d\varphi \tag{35}$$

But φ was chosen as the angle off the x axis so the integral of the sin $(ky\sin\varphi)$ function from $-\Delta\varphi$ to $\Delta\varphi$ is zero.
Therefore

$$F(\Delta\varphi)=\frac{1}{\Delta\varphi}\int_{0}^{\Delta\varphi}\cos(ky\sin\varphi)\exp(-ikx\cos\varphi)\,d\varphi \tag{36}$$

A limiting case that is interesting to consider is that of a very narrow beam ($\Delta\varphi \ll 1.0$). Then φ is small and equation 36 is approximately

$$F(\Delta\varphi) \cong \frac{1}{2\Delta\varphi}\int_{-\Delta\varphi}^{\Delta\varphi} \cos ky\varphi \exp\left[-ikx\left(1-\frac{\varphi^2}{2}\right)\right] d\varphi$$

$$= \frac{\exp(-ikx)}{2\Delta\varphi}\int_{-\Delta\varphi}^{\Delta\varphi}\left[\exp\left(\frac{ikx\varphi^2}{2}\right)\right]\left[\frac{\exp(iky\varphi)+\exp(-iky\varphi)}{2}\right] d\varphi$$

$$= \frac{\exp(-ikx)}{4\Delta\varphi}\left(\int_{-\Delta\varphi}^{\Delta\varphi}\exp\left\{\frac{ikx}{2}\left[\left(\varphi+\frac{y}{x}\right)^2-\left(\frac{y}{x}\right)^2\right]\right\} d\varphi\right. \tag{37}$$

$$\left. + \int_{-\Delta\varphi}^{\Delta\varphi}\exp\left\{\frac{ikx}{2}\left[\left(\varphi-\frac{y}{x}\right)^2-\left(\frac{y}{x}\right)^2\right]\right\} d\varphi\right)$$

$$= \frac{1}{4\Delta\varphi}\exp\left\{-ikx\left[1+(1/2)\left(\frac{y}{x}\right)^2\right]\right\}\left\{\int_{-\Delta\varphi}^{\Delta\varphi}\exp\left[\frac{ikx}{2}\left(\varphi+\frac{y}{x}\right)^2\right] d\varphi\right.$$

$$\left. + \int_{-\Delta\varphi}^{\Delta\varphi}\exp\left[\frac{ikx}{2}\left(\varphi-\frac{y}{x}\right)^2\right] d\varphi\right\}$$

Transforming variables so that $v_{\pm}^2 = (2x/\lambda)(\varphi \pm y/x)^2$ and being careful in rearranging terms according to appropriate limits, equation 37 can be written as follows:

$$F(\Delta\varphi) = \frac{\exp\left\{ikx\left[1+(1/2)\left(\frac{y}{x}\right)^2\right]\right\}}{2\sqrt{\frac{2x}{\lambda}}\Delta\varphi}\left(\int_0^{v_+}\cos\frac{\pi}{2}v^2 dv + \int_0^{v_-}\cos\frac{\pi}{2}v^2 dv\right.$$

$$\left. + i\int_0^{v_+}\sin\frac{\pi}{2}v^2 dv + i\int_0^{v_-}\sin\frac{\pi}{2}v^2 dv\right) \tag{38}$$

which is the convenient form since the integrals are the Fresnel integral which is commonly tabulated. To arrive at this form, note that both the cosine and sine terms are even functions.

For station separation in the x direction only (stations located along the direction of propagation) y is zero and the equation simplifies to just two Fresnel integrals. The result is plotted as the black curves corresponding to various beam widths, $\Delta\varphi$, in figure 10. Note that the

left-hand scale is to be used and its great expansion shows immediately that coherence falls off very slowly for separations along the direction of propagation even for fairly large beam widths.

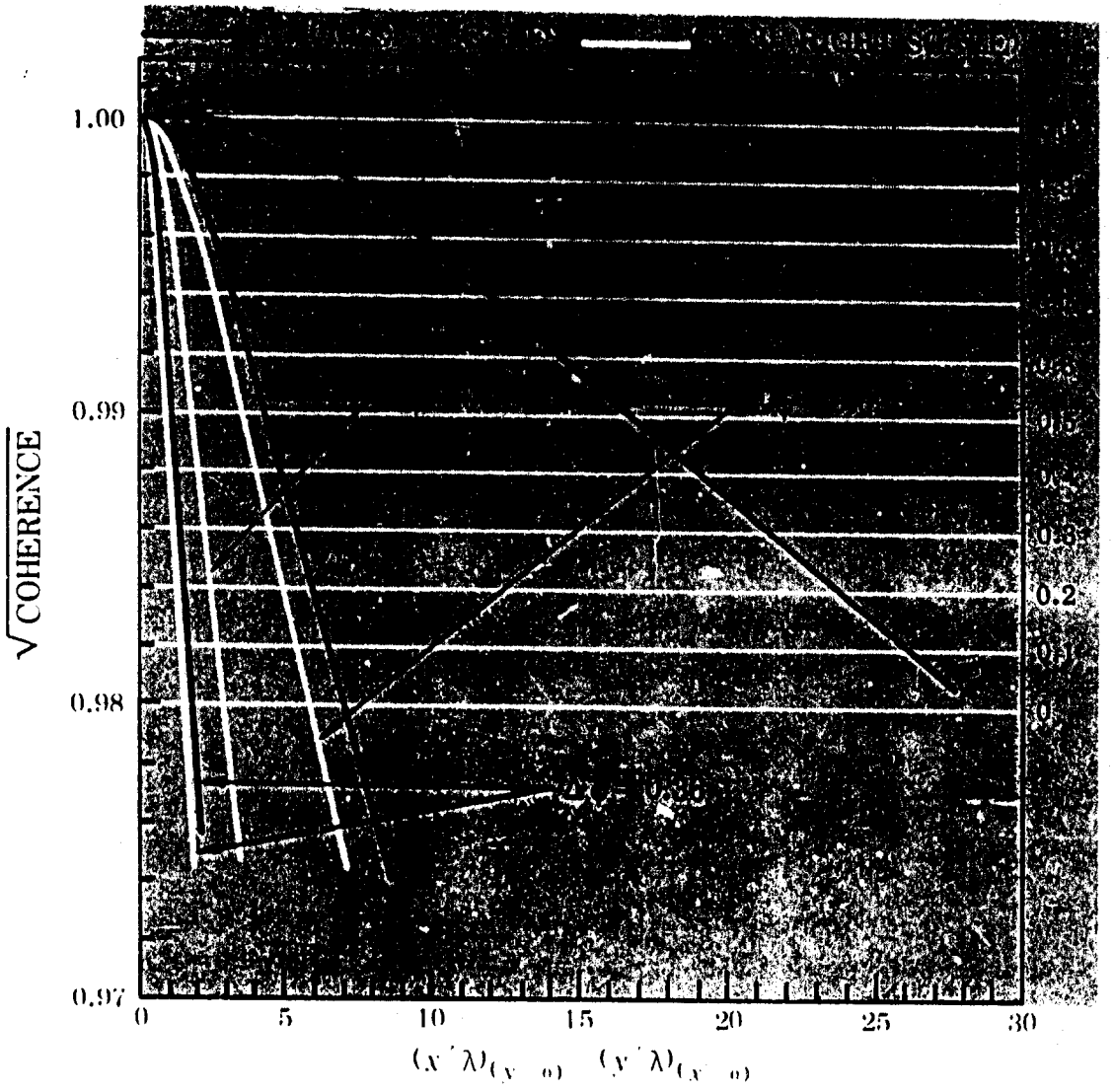

Figure 10. Dependence of $\sqrt{\text{coherence}}$ on recorder separation and wavelength. x is separation in the direction of propagation. y is separation perpendicular to the direction of propagation.

For station separation in the y direction, $x = 0$. (The line of stations is then perpendicular to the direction of propagation.) For this case, it is convenient to return to equation 36 so that with $x = 0$, we have

$$|F(\Delta\varphi)| = \frac{1}{\Delta\varphi}\left|\int_0^{\Delta\varphi} \cos(ky\sin\varphi)\, d\varphi\right| \tag{39}$$

which for $\Delta\varphi \ll 1$ gives

$$|F(\Delta\varphi)| = \left|\frac{\sin k_y \Delta\varphi}{k_y \Delta\varphi}\right| \tag{40}$$

For $\Delta\varphi \ll 1.0$, $\Delta\varphi \cong \sin\Delta\varphi$ so $k\Delta\varphi \cong k_y = 2\pi/\lambda_y$ (see fig. 9). Therefore the $\sqrt{\text{coherence}}$ provides a measure of the dimension perpendicular to the direction of propagation, i.e., the "long-crestedness" of the waves.

The $\sqrt{\text{coherence}}$ for separation in the y direction is shown plotted as the white curves in figure 10 and the right-hand scale should be used. It is immediately seen that the coherence falls off much more rapidly (for a given beam width) for station separation perpendicular to the direction of propagation than for separation along the propagation direction.

The general situation when $E(\omega)$ is independent of φ and $\Delta\varphi \ll 1.0$ is summarized in figure 11 where the $\sqrt{\text{coherences}}$ for arbitrary directions of separation are shown for an assumed station separation of $L/\lambda = \sqrt{2}$.

The other limiting case that is interesting to consider is that of nondirectional radiation (uniform in all directions) so that $\Delta\varphi = \pi$. Then we see from equation 39 that

$$|F(ky)| = \frac{1}{\pi}\left|\int_0^{\pi} \cos(ky\sin\varphi)\, d\varphi\right| = |J_0(ky)| \tag{41}$$

The $\sqrt{\text{coherence}}$ then falls off with station separation ($y = L$) as the $|J_0(ky)|$ curve shown in figure 12. The coherence becomes negligible in all directions when the separation is about 0.4 wavelength.

If the recorders are located very near a large source region it is of interest to consider the integral taken over the whole half-plane that includes the source ($-\pi/2 \leq \varphi \leq \pi/2$). Then

$$F(kx, ky) = \frac{1}{\pi}\int_{-\pi/2}^{\pi/2} \cos(ky\sin\varphi)\exp(-ikx\cos\varphi)\, d\varphi \tag{42}$$

For separation along the x direction ($y = 0$) the integral is again $J_0(ky)$ since on changing the variable φ to γ, where $\gamma = (\pi/2) - \varphi$

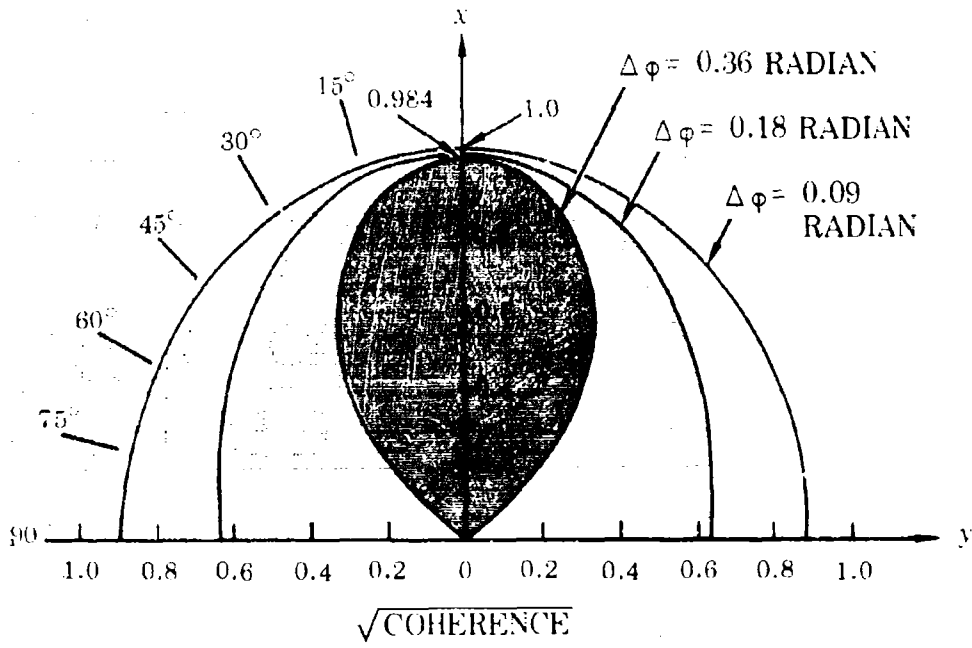

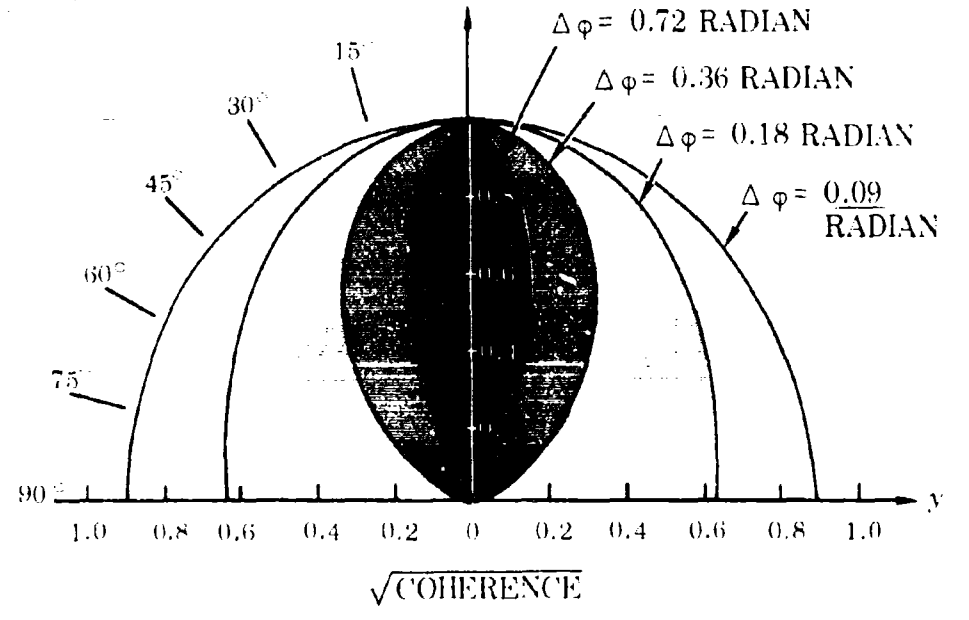

Figure 11. Contours of $\sqrt{\text{coherence}}$ as angle between direction of station separation and direction of propagation (x direction) is changed. Assumed station separation is $\sqrt{2}$ wavelengths. Top, rigorous plot from equation 38. Bottom, corresponding plot from equation 40 using only y component of separation. Excellent agreement shows that coherence depends almost exclusively on the component of station separation perpendicular to the direction of propagation.

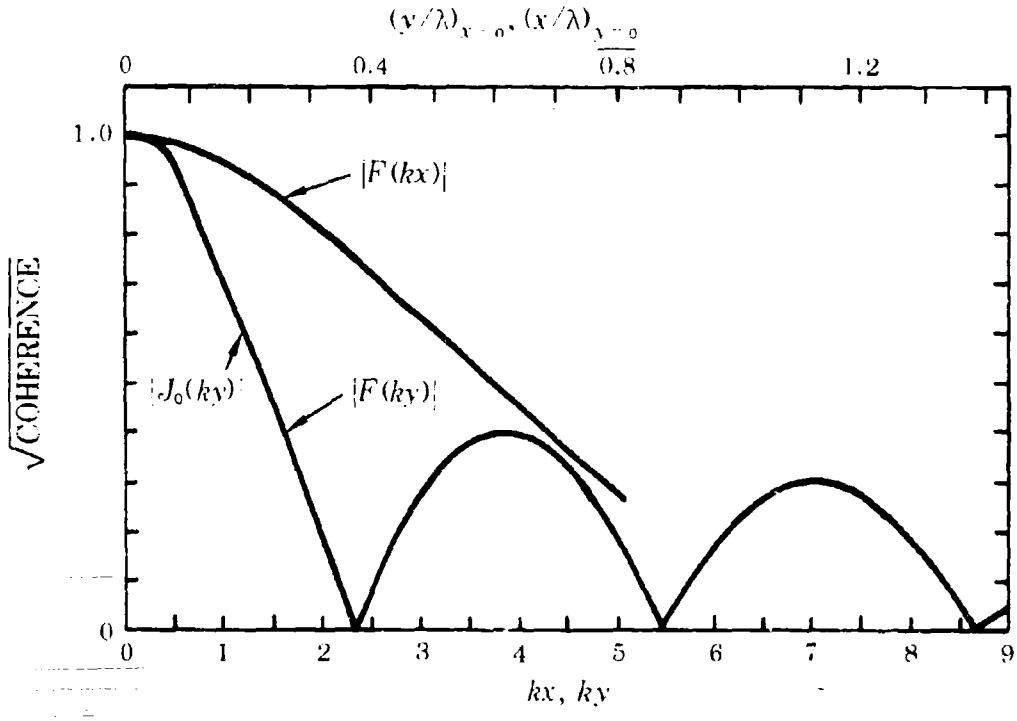

Figure 12. Dependence of $\sqrt{\text{coherence}}$ on recorder separation and wavelength when the integration extends over all angles (isotropic case). $\sqrt{\text{coherence}}$ then decreases equally for all directions of separation according to $J_0(ky)$. When integration is over the whole half-plane of the source, $\sqrt{\text{coh}}$ falls off according to $|F(kx)|$ for separation in the x direction and according to $|F(ky)|$ for separation in the y direction.

$$F(ky) = \frac{1}{\pi}\int_0^{\pi} \cos(ky\cos\gamma)\, d\gamma = J_0(ky) \tag{43}$$

For separation along the x direction ($y = 0$)

$$F(kx) = \frac{1}{\pi}\int_{-\pi/2}^{\pi/2} \cos(kx\cos\varphi)\, d\varphi - \frac{i}{\pi}\int_{-\pi/2}^{\pi/2} \sin(kx\cos\varphi)\, d\varphi \tag{44}$$

By a transformation similar to that above (i.e., letting $\gamma = (\pi/2) - \varphi$ the first integral is

$$\frac{1}{\pi}\int_0^{\pi} \cos(kx\sin\gamma)\, d\gamma = J_0(kx) \tag{45}$$

The second integral is more complicated. Again transforming to a variable ranging from limits of 0 to π,

$$\frac{1}{\pi}\int_{-\pi/2}^{\pi/2}\sin(kx\cos\varphi)\,d\varphi=\frac{1}{\pi}\int_{0}^{\pi}\sin(kx\sin\gamma)\,d\gamma$$

The integrand $\sin(kx\sin\gamma)$ can be represented as a series (see, for example, ref. 13) so that

$$\frac{1}{\pi}\int_{0}^{\pi}\sin(kx\sin\gamma)\,d\gamma=\frac{2}{\pi}\sum_{n=0}^{\infty}J_{2n+1}(kx)\int_{0}^{\pi}\sin\left[(2n+1)\gamma\right]d\gamma$$

$$=\frac{2}{\pi}\sum_{n=0}^{\infty}\left[J_{2n+1}(kx)\left(\frac{2}{2n+1}\right)\right] \tag{46}$$

$$=\frac{4}{\pi}\left[J_1(kx)+\frac{J_3(kx)}{3}+\frac{J_5(kx)}{5}\cdots\right]$$

So for separations in the x direction $F(kx)$ is simply evaluated from

$$F(kx)=J_0(kx)-\frac{4}{\pi}i\left[J_1(kx)+\frac{J_3(kx)}{3}+\frac{J_5(kx)}{5}\cdots\right]$$

For $kx \ll 2\pi$ only a few terms are needed and the Bessel functions are conveniently tabulated in many places. $F(kx)$ is shown in figure 12 for $kx < 2\pi$.

Sample Problem Applying Cross-Spectrum Analysis to Spatially Separated Recordings

Figure 13 shows the configuration of an experiment reported by Gossard and Paulson [14]. Radio waves at a frequency of 44.3 kHz were reflected off the lower ionosphere and received at a triangle of spaced receivers. The receiver sites are indicated by MW, OR, and GL and their separations in kilometers are shown on the figure. It is assumed that the

movement of ionospheric irregularities in electron density causes a similar movement of the diffraction pattern of reflected radio waves received at the surface of the earth. The observed movement of the diffraction pattern is then compared with ionospheric wind measurements obtained by photographing the drift of chemiluminescent trails produced by contaminants injected into the lower ionosphere by a gun-launched projectile[15] located near midpath.

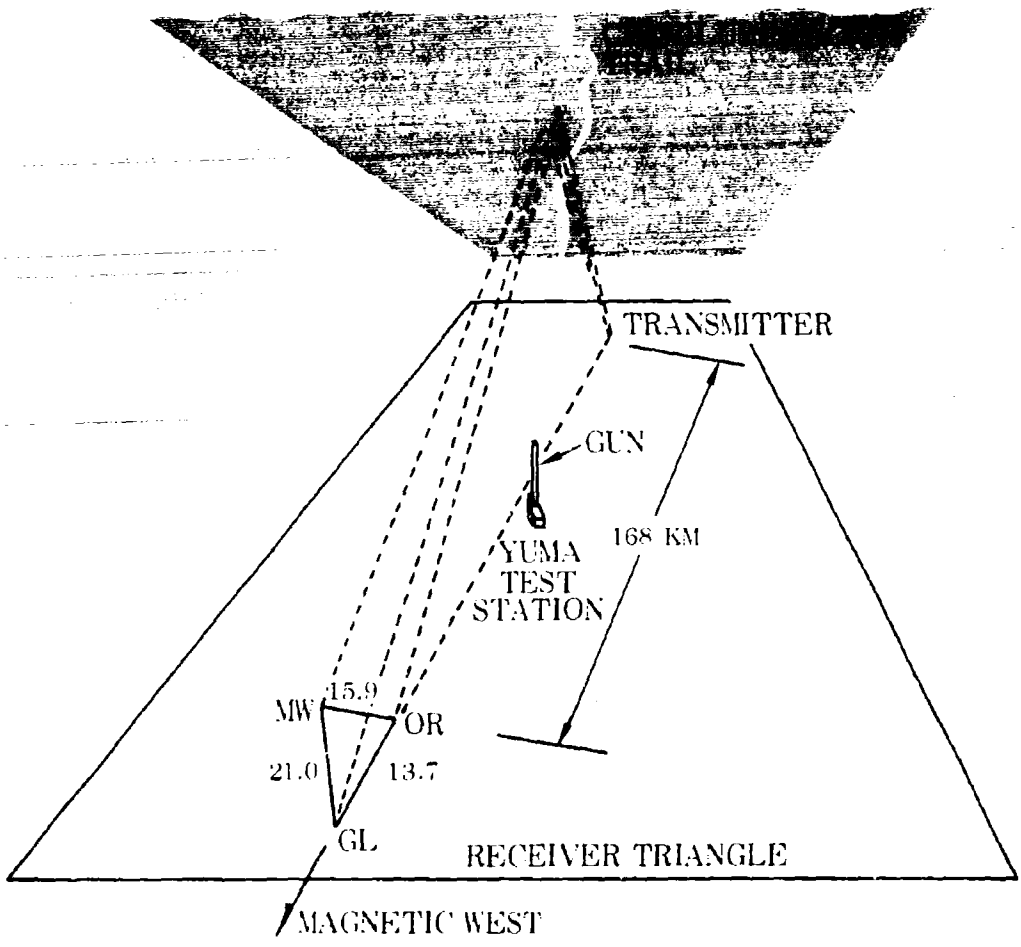

Figure 13. Perspective drawing showing geometry of multiple receiver experiment to measure movement of irregularities of electron density in the ionosphere. Length units in MW, OR, GL receiver triangle are kilometers. Transmitter is near Sentinel, Arizona. Data are analyzed for ionospheric wave motions, using cross-spectrum technique.

Sample records of amplitude fluctuations observed at the three receiver sites on 13 and 14 June 1966 are shown in figure 14, together with height contours of the 500-mb pressure surface two days earlier. The time lag is roughly in accord with the theoretical time required for energy to flow from the troposphere to the ionosphere for typical atmospheric wind and temperature distributions. Therefore it is of interest to inquire whether the direction of propagation of the diffraction pattern and its "beam width" are compatible with such a source.

A cross-spectrum analysis of the records of the three stations was performed, and it was found that the velocity of propagation of a prominent spectral line with a period of 5.8 minutes was 47 mps toward a direction 14 degrees west of north. The wave crests were therefore only about 12° from alignment with the MW-GL line of separation of receivers. The indicated coherence between MW and GL for this spectral line was about 0.44. The wavelength of this wave component was 17 km and the station separation was 21 km, so $L/\lambda = 1.24$. Figure 10 shows that $\Delta\varphi$ is therefore about 0.3 radian so that the transverse wavelength is about triple that normal to the crests. We therefore conclude that the direction of propagation of the 5.8-minute spectral line is compatible with the observed position of the tropospheric disturbance and the "beam width" indicated by the coherence analysis is appropriate to an extended source.

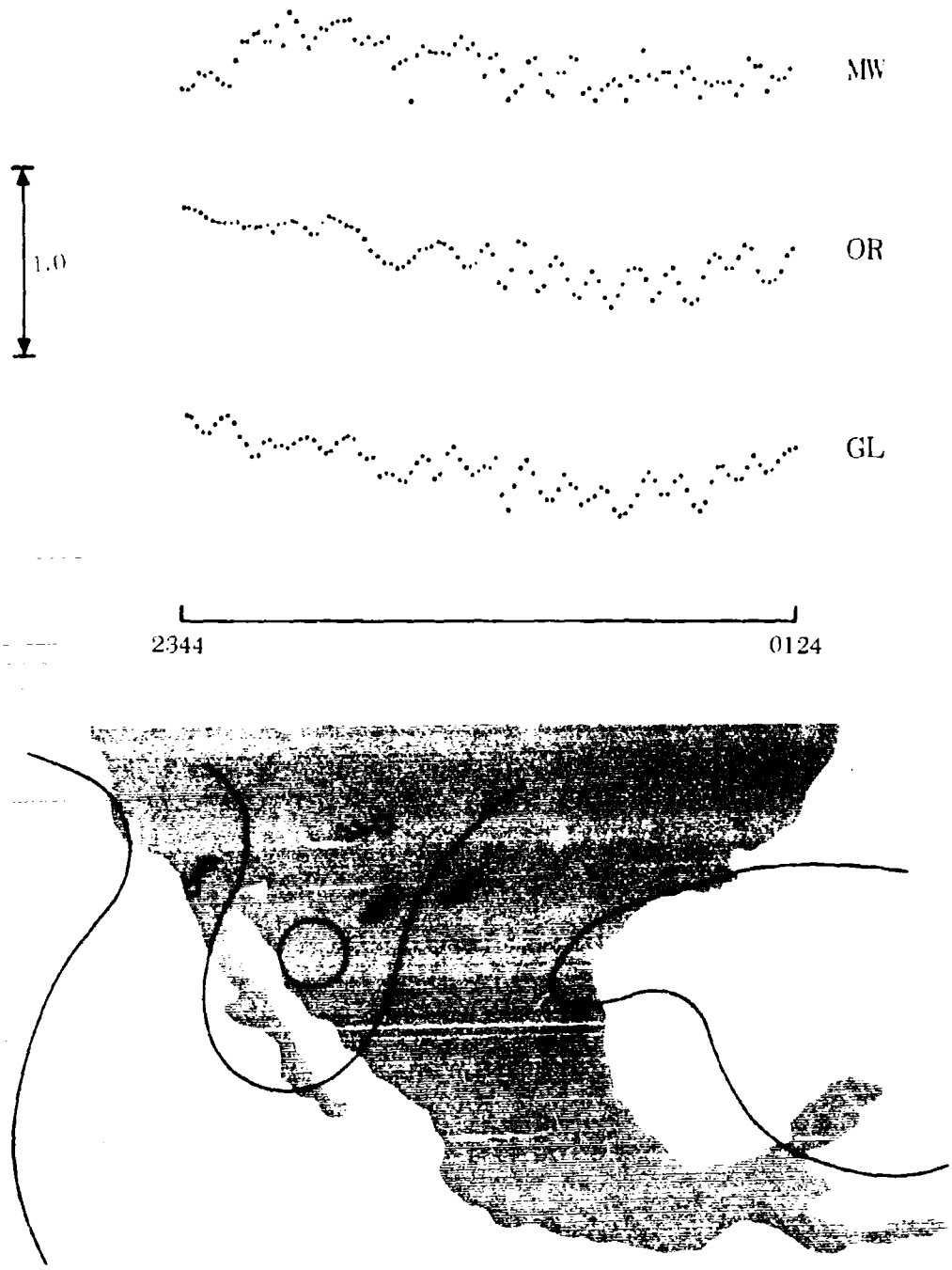

Figure 14. Sample record of radio amplitude fluctuations (top) produced by wave motions in the lower ionosphere. Radio frequency is 44.3 kHz, time is MST, and amplitudes are normalized to the record average. The weather map (bottom) shows height contours of the 500-mb pressure surface two days earlier. The white triangle shows the location of the experimental site.

REFERENCES

1. Taylor, G.I., "Diffusion by Continuous Movements," *London Mathematical Society. Proceedings*, Series 2, v.20, p.196-212, 1922

2. Wiener, N., "Generalized Harmonic Analysis," *Acta Mathematica*, v.55, p.117-258, 1930

3. Blackman, R.B. and Tukey, J.W., *The Measurement of Power Spectra*, Dover Publications, 1958

4. Panofsky, H.A. and Brier, G.W., *Some Applications of Statistics to Meteorology*, Pennsylvania State University, 1958

5. Gossard, E.E., "Power Spectra of Temperature, Humidity and Refractive Index From Aircraft and Tethered Balloon Measurements," *Institute of Radio Engineers. Transactions: Antennas and Propagation*, v.AP-8, p.186-201, March 1960

6. Munk, W.H., Snodgrass, F.E. and Tucker, M.J., "Spectra of Low Frequency Ocean Waves," *Scripps Institution of Oceanography. Bulletin*, v.7, p.283-362, 16 October 1959

7. Goodman, N.R., *On the Joint Estimation of the Spectra, Cospectrum and Quadrature Spectrum of a Two-Dimensional Stationary Gaussian Process*, (Ph.D. Thesis, Princeton University), 1957 (AD 134919)

8. Goodman, N.R., "Statistical Analysis Based on a Certain Multivariate Complex Gaussian Distribution (An Introduction)," *Annals of Mathematical Statistics*, v.34, p.152-177, March 1963

9. Madden, T., "Spectral, Cross-Spectral and Bispectral Analysis of Low Frequency Electromagnetic Data," p.429-450 in NATO Advanced Study Institute, Homburg vor der Höhe, 1963, *Natural Electromagnetic Phenomena Below 30 kc/s: Proceedings of a NATO Advanced Study Institute Held in Bad Homburg, Germany, July 22 - August 2, 1963*, Plenum Press, 1964

10. Alexander, M.J. and Vok, C.A., *Tables of the Cumulative Distribution of Sample Multiple Coherence*, 9 Vols., Canoga Park, California,

Rocketdyne Division of North American Aviation, 1963 (Rocketdyne Research Report 63-37)

11. Noonkester, V.R., "E- and F-Region Variations Near Periods of 27 and 15 Days at Washington, D.C.," *Journal of Atmospheric and Terrestrial Physics,* v.27, p.605-616, May 1965

12. Cox, C.S., "Internal Waves, Part II," p.752-763 in Hill, M.N., *The Sea; Ideas and Observations on Progress in the Study of the Seas, v.1: Physical Oceanography*, Interscience Publishers, 1962

13. U.S. National Bureau of Standards, *Handbook of Mathematical Functions,* 1964 (NBS. Applied Mathematics Series, 55)

14. Gossard, E. and Paulson, M., "A Case Study of a Periodic Structure in the Atmosphere Near the 90-km Level," *Journal of Atmospheric and Terrestrial Physics* (In press)

15. Murphy, C.H. and others, "Ionospheric Winds Measured by Gun-Launched Projectiles," *Journal of Geophysical Research*, v.71, p.4535-4544, 1 October 1966

APPENDIX A: CONVENIENT NUMERICAL FILTERS

One of the simplest mathematical filters is a running average. Consider the effect of a running average on the Fourier component

$$x = A \cos \frac{2\pi t}{T} \tag{A-1}$$

When the running average extends from $-t_a/2$ to $+t_a/2$ the average is taken symmetrically about the maximum of a cosine curve, and we have for the running average, $\bar{x}$

$$\bar{x} = \frac{A}{t_a} \int_{-t_a/2}^{t_a/2} \cos \frac{2\pi t}{T}\, dt \tag{A-2}$$

Integration of (A-2) gives the filter response $F(T)$ as

$$F(T) = \frac{T}{\pi t_a} \sin \frac{\pi t_a}{T} \tag{A-3}$$

The power at each period T is reduced according to

$$F^2(T) = \left(\frac{T}{\pi t_a}\right)^2 \sin^2 \left(\frac{\pi t_a}{T}\right) \tag{A-4}$$

Figure A1 shows $F^2(T)$ or the filter response of the simple running average as the white curve. The high frequencies are suppressed but $F^2(T)$ contains large side lobes, the first of which has an amplitude of about one-tenth of the main lobe. This filter is undesirable because side-lobe frequencies would be accented in a spectral analysis.

A more desirable filter results from a triangularly weighted average given by

$$\bar{x} = \frac{A \int_0^{t_a/2} \left(\frac{t_a}{2} - 1\right) \cos \frac{2\pi}{T} t\, dt}{\int_0^{t_a/2} \left(\frac{t_a}{2} - 1\right) dt} \tag{A-5}$$

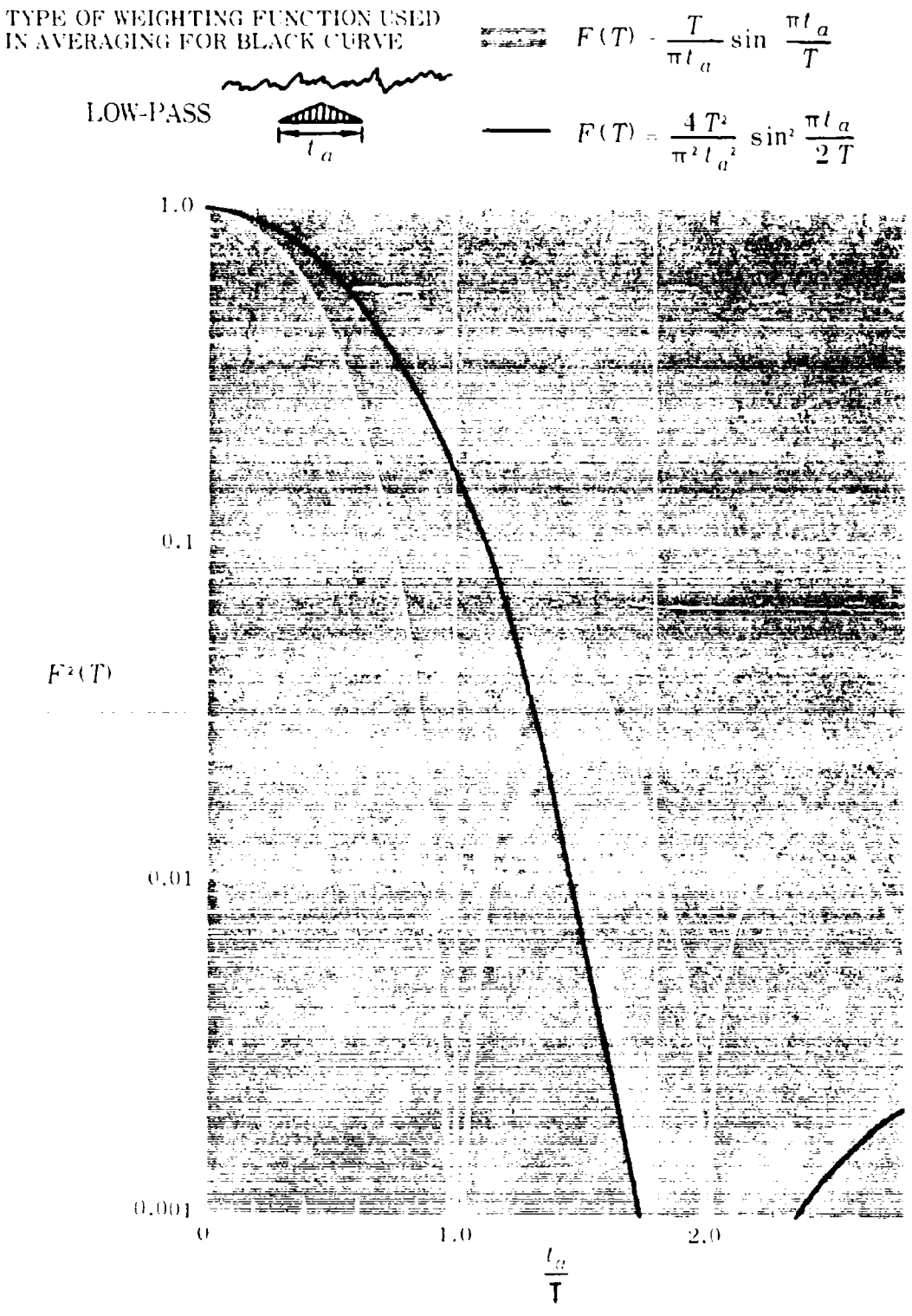

Figure A1. Low pass filter response curves for two simple numerical filters, based on equations shown.

with a filter response

$$F(T) = \left(\frac{2T}{\pi t_a}\right)^2 \sin^2 \frac{\pi t_a}{2T} \qquad \text{(A-6)}$$

$F^2(T)$ from equation A-6 is shown as the black curve in figure A1. The function has smaller side lobes than that of the filter given by equation A-4, but the frequency cutoff is less abrupt.

The low-pass filter (eq. A-6) can be used as a high-pass filter by subtracting the filtered data from the unfiltered (raw) data. The response of this high-pass filter is given in figure A2 calculated using A-7. The filter can be written for digitized data as the right-hand term of the following equation where $y_i = x_i - \bar{x}$ and $m = \frac{1}{2}\left(\frac{t_a}{\Delta t} - 1\right)$

$$y_i = x_i - \frac{1}{m^2}\left[x_{i-m+1} + 2x_{i-m+2} + \cdots + (m-1)x_{i-1} + mx_i + (m-1)x_{i+1} + \cdots + 2x_{i+m-2} + x_{i+m-1}\right] \qquad \text{(A-7)}$$

where i is the i-th value in the time series and m is the half-width of the triangularly weighted averaging interval. The sample size is reduced by $2m$ (m points are lost both at the beginning and the end of the sample) and the mean of the filtered data is zero. Other filters can be designed but those given by equation A-4 or A-6 are convenient and adequate for many purposes.

The data shown in figure 2 were filtered using an m of 100 to remove the lower frequencies. This filter reduced the amplitude of the annual cycle of $f\bar{E}$ to about 0.05 of its original value while leaving components having periods less than 100 days essentially unchanged. The filtered data are shown as the bottom record of figure 2. Because the first and last 100 data values were eliminated by the filter, the raw data extended 100 days before and 100 days after days numbered 0 and 180, respectively.

Examination of the filtered data in figure 2 clearly shows that the higher frequencies are almost unaffected by the filter. The reduction in the amplitude of the component having the period of the annual cycle is

obvious but no obvious reduction is noted in periods of 100 to 200 days.

Analysis of the filtered $\overline{fE}$ should not extend to periods much greater than 100 days. This study used a sample size of 2722 (days). For the Fourier component having a period of 100 days, $\overline{fE}$ has 27 possible cycles in the record. Twenty-seven cycles are considered adequate and are considered to be within the large sample category.

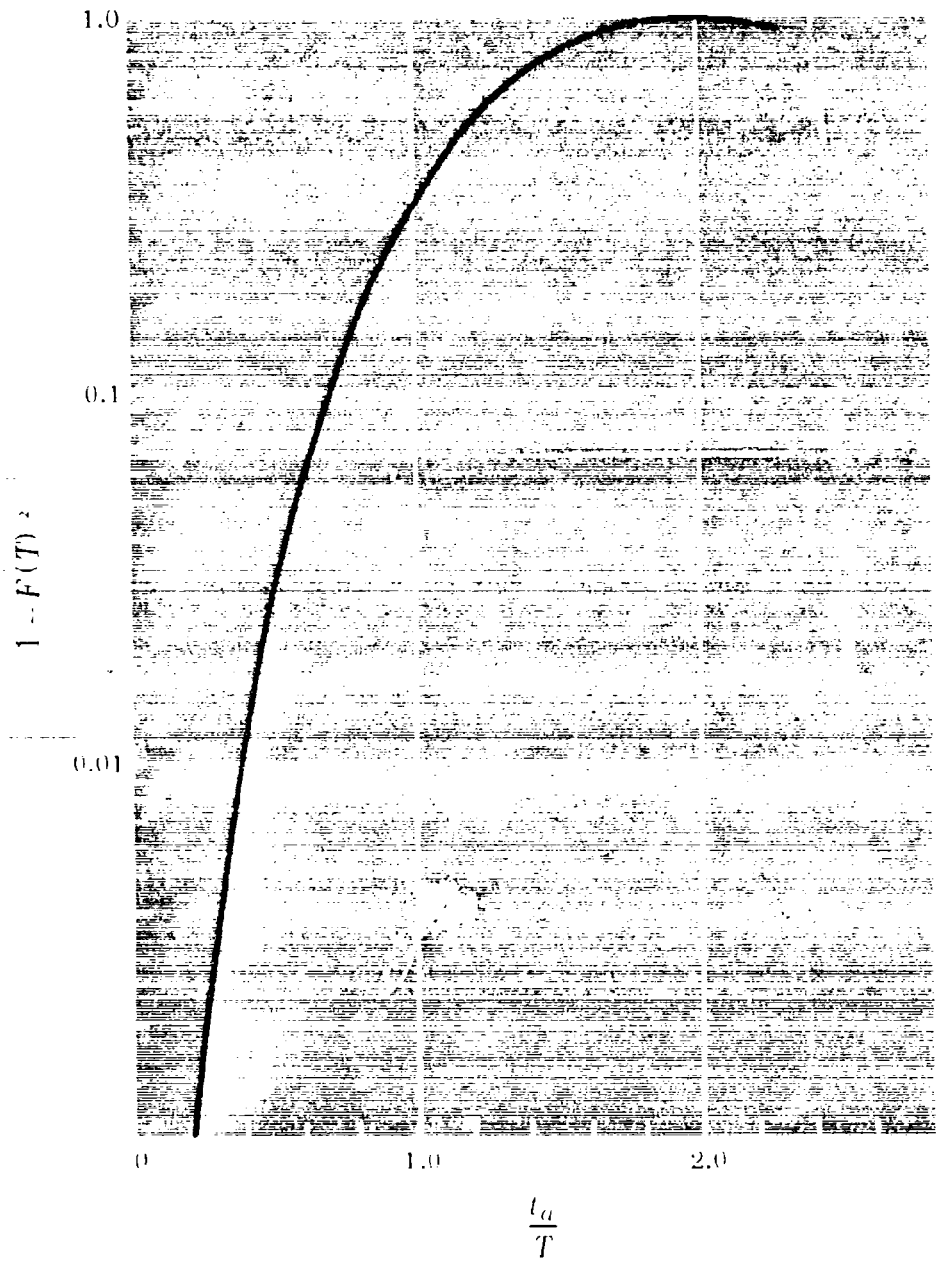

Figure A2.—High-pass filter response resulting from use of equation A-7.

APPENDIX B: USEFUL FORMULAE FOR DIGITAL COMPUTATION OF SPECTRA

Auto-Covariance:

$$R_{11}(p) = \frac{1}{N-p} \sum_{i=1}^{i=N-p} (x_1 - \bar{x}_1)_i (x_2 - \bar{x}_2)_{i+p}$$

where

$$\bar{x}_1 = \frac{1}{N-p} \sum_{i=1}^{i=N-p} x_i, \quad \bar{x}_2 = \frac{1}{N-p} \sum_{i=1+p}^{i=N} x_{i+p}$$

Cross-Covariance Function:

$$R_{12}(p) = \frac{1}{N-p} \sum_{i=1}^{i=N-p} (x - \bar{x})_i (y - \bar{y})_{i+p}$$

where

$$\bar{x} = \frac{1}{N-p} \sum_{i=1}^{i=N-p} x_i, \quad \bar{y} = \frac{1}{N-p} \sum_{i=1+p}^{i=N} y_{i+p}$$

Power Spectrum (per cycle per unit time):

$$E(f) = 4\Delta t \delta \sum_{p=0}^{p=m} R_{11}(p) \cos \frac{\pi p h}{m} \text{ where } \delta = \begin{cases} 1/2 \text{ for } p = 0, m \\ 1 \text{ for } 0 < p < m \end{cases}$$

Power Spectrum (Includes Hanning filter window)(per cycle per unit time):

$$E(f) = 2\Delta t \left[R_{11}(0) + \sum_{p=1}^{p=m-1} R_{11}(p) \left(1 + \cos \frac{\pi p}{m}\right) \cos \frac{\pi p h}{m} \right]$$

Cross-Power Spectra:

$$C(f) = 2\Delta t\left[R_{12}(0) + \sum_{p=1}^{p=m-1} \frac{R_{12}(p) + R_{12}(-p)}{2}\left(1 - \cos\frac{\pi p}{m}\right)\cos\frac{\pi ph}{m}\right]$$

$$Q(f) = 2\Delta t\left[\sum_{p=1}^{p=m-1} \frac{R_{12}(p) - R_{12}(-p)}{2}\left(1 + \cos\frac{\pi p}{m}\right)\sin\frac{\pi ph}{m}\right]$$

Bandwidth of Analysis:

$$\Delta f = (2m\Delta t)^{-1}$$

Highest Frequency in Digital Analysis (Nyguist frequency):

$$f_{max} = (2\Delta t)^{-1}$$

$$\text{Coherence}\ (f) = \frac{C^2(f) + Q^2(f)}{E_1(f)\,E_2(f)}$$

Phase Cross Spectrum:

$$\tan\omega\tau = \tan 2\pi f\tau = \frac{Q(f)}{C(f)}$$

UNCLASSIFIED
Security Classification

DOCUMENT CONTROL DATA - R & D

(Security classification of title, body of abstract and indexing annotation must be entered when the overall report is classified)

1. ORIGINATING ACTIVITY (Corporate author)

Naval Electronics Laboratory Center
San Diego, California

2a. REPORT SECURITY CLASSIFICATION

UNCLASSIFIED

2b. GROUP

3. REPORT TITLE

A Guide to Digital Computation and Use of Power Spectra and Cross-Power Spectra

4. DESCRIPTIVE NOTES (Type of report and inclusive dates)

5. AUTHOR(S) (First name, middle initial, last name)

Earl E. Gossard and Virgil R. Noonkester

6. REPORT DATE	7a. TOTAL NO. OF PAGES	7b. NO. OF REFS
3 November 1967 (Rev. April 1968)	51	15

8a. CONTRACT OR GRANT NO.	9a. ORIGINATOR'S REPORT NUMBER(S)
b. PROJECT NO.	Technical Document 20 TD 20 (Rev.)
c.	9b. OTHER REPORT NO(S) (Any other numbers that may be assigned this report)
d.	None

10. DISTRIBUTION STATEMENT

This document is subject to special export controls and each transmittal to foreign governments or foreign governments or foreign nationals may be made only with prior approval of Naval Electronics Laboratory Center.

11. SUPPLEMENTARY NOTES	12. SPONSORING MILITARY ACTIVITY
None	Naval Electronics Laboratory Center

13. ABSTRACT

This document attempts to bring together a description of the methodology of spectrum and cross spectrum analysis which is scattered in the scientific literature. The digital formulation required by most engineers and applied physicists are given. Elementary derivations of the basic formulae are given. The various errors that may contaminate the analysis are discussed together with the confidence limits applicable to samples of finite length. Examples are given illustrating the application and the step-by-step procedure for obtaining spectra and cross spectra. Two very different applications of cross-spectrum analysis are described, and the significance of cross-power and coherence is discussed.

DD FORM 1 NOV 65 1473 (PAGE 1)

S/N 0101-807-6801

UNCLASSIFIED
Security Classification

14 KEY WORDS	LINK A		LINK B		LINK C	
	ROLE	WT	ROLE	WT	ROLE	WT
Power Spectra Computation						
Cross-Power Spectra Computation						